minerals

MDPI

Article

Comparison of Fuzzy and Neural Network Computing Techniques for Performance Prediction of an Industrial Copper Flotation Circuit

Ivana Jovanović [1,*], Fardis Nakhaei [2,*], Daniel Kržanović [1], Vesna Conić [1] and Daniela Urošević [1]

1 Mining and Metallurgy Institute Bor, Zeleni Bulevar 35, 19210 Bor, Serbia
2 School of Chemical and Minerals Engineering, North West University, Potchefstroom 2531, South Africa
* Correspondence: ivana.jovanovic@irmbor.co.rs (I.J.); 36598704@mynwu.ac.za (F.N.)

Abstract: This paper presents the development and validation of five different soft computing methods for flotation performance prediction: (1) two models based on fuzzy logic (Mamdani and Takagi-Sugeno fuzzy inference system) and (2) three models based on artificial neural networks. Copper content in the ore feed, collector dosage in the rougher and the scavenger flotation circuits, slurry pH in the rougher flotation circuit and frother consumption were selected as input parameters to estimate the copper grade and recovery of final concentrate, as well as the copper content in the final tailings of the flotation plant. The training and evaluation of the proposed models were performed on the basis of real process data collected by the multiannual monitoring of industrial flotation plant operation in "Veliki Krivelj Mine". The results showed that the proposed soft computing-based models well describe the behavior of the industrial flotation plant in a wide range of circumstances. Among the proposed algorithms, artificial neural networks gave the most accurate predictions for the final copper concentrate grade and recovery (R^2 = 0.98 and R^2 = 0.99, respectively) and copper content in final tailings (R^2 = 0.87). At some points, fuzzy logic models are almost equally efficient, but artificial neural networks had lower values for all error functions.

Keywords: copper flotation; fuzzy logic; artificial neural network; mathematical modeling

check for updates

Citation: Jovanović, I.; Nakhaei, F.; Kržanović, D.; Conić, V.; Urošević, D. Comparison of Fuzzy and Neural Network Computing Techniques for Performance Prediction of an Industrial Copper Flotation Circuit. *Minerals* **2022**, *12*, 1493. https://doi.org/10.3390/min12121493

Academic Editor: Hyunjung Kim

Received: 15 September 2022
Accepted: 16 November 2022
Published: 23 November 2022

Publisher's Note: MDPI stays neutral with regard to jurisdictional claims in published maps and institutional affiliations.

Copyright: © 2022 by the authors. Licensee MDPI, Basel, Switzerland. This article is an open access article distributed under the terms and conditions of the Creative Commons Attribution (CC BY) license (https://creativecommons.org/licenses/by/4.0/).

1. Introduction

In the mining industry, the separation of valuable minerals from raw ores is carried out using the flotation process to obtain qualified concentrate and to eliminate tailings. Recovery and grade of the concentrate are the important metallurgical factors of the flotation process. In an industrial flotation plant, the online prediction of the metallurgical factors is costly and time-consuming. Since the flotation is a nonlinear process, modeling, automatic monitoring and control of the industrial plants based on the metallurgical factors have met with limited success at the present time. Furthermore, the process models based on classical experimental methods do not provide sufficiently efficient results when it comes to such complex systems [1]. To overcome these difficulties, the use of statistical and artificial intelligence methods for control and monitoring purposes of the flotation process has been developed [2]. Therefore, soft sensors based on problem-solving technologies such as fuzzy logic and neural networks (NNs) emerged as perspective alternatives to the classical modeling approaches. These methods, unlike the conventional mathematical techniques, exhibit a certain tolerance to the imprecision and uncertainty of technological parameters in the description of real systems [3–6].

The most commonly used soft computing methods in the modeling of flotation process are different types of NNs due to their acceptable accuracy, robustness, simplicity and nonlinearity [7–9]. NNs use very powerful computational techniques for modeling the complex nonlinear processes. Among them, a frequently used NN is a multilayer perceptron (MLP) based on which models for predicting various flotation parameters have been developed. For example, Al-Thyabat [10] examined the suitability of different MLP architectures by considering the influence of three input parameters (mean particle size in the feed slurry, collector dosage and impeller rotation speed) on the grade and recovery of the concentrate obtained by the phosphate flotation process. Similarly, Farghaly et al. [11] used an artificial neural network (ANN) model to investigate the effect of flotation time, collector dosage, frother dosage and impeller speed on the grade and recovery of coal concentrate. Jorjani et al. [12] formed two MLP architectures (7-10-3-1) and (5-30-2-1), for predicting the recovery and grade of the coal concentrate, respectively.

Nakhaei et al. [13–15] proposed several ANN models for predicting the contents and recoveries of copper and molybdenum in the column flotation concentrate. The authors concluded that NNs proved to be a superior technique compared to the regression models. The same conclusion was obtained by other researchers comparing the statistical methods and techniques based on MLP for the modeling of copper minerals' flotation process [16,17]. More recently, the researchers proposed ANN models for the prediction of the phosphate concentrate grade [18], and removal Cu (II) ion in flotation systems [19].

Some authors have also considered the application of other types of NNs. For example, Gholami et al. [20] used two types of recurrent neural networks (RNN)—Long short-term memory network (LSTM) and Gated recurrent unit network (GRU)—to predict the grade and recovery of copper concentrate within different operating conditions. They compared the results obtained by the RNN with models based on classical NN and random forest methods. They demonstrated that the RNN models have a better prediction ability. The potential of RNNs was also considered by Nakhaei and Irannajad [15], where they demonstrated good abilities to predict the content and recovery of Cu and Mo in the final concentrate obtained in the flotation column (correlation coefficient greater than 0.8).

There are also numerous studies for the application of NN in the models related to the identification, categorization and interpretation of flotation froth images [21–30]. These models typically use extracted features from flotation froth images. In recent times, convolutional neural networks are increasingly being used to model the flotation process, especially when it comes to the classification and feature recognition of froth images [31–35].

Fuzzy logic supports the ability of the human mind to effectively express a way of reasoning that is more approximate than exact. It is a computation and reasoning system where the objects of computation and reasoning are classes with fuzzy limitations. Fuzzy logic system allows analysis for modeling complex and poorly defined systems in which linguistic expressions are used rather than numerical variables [36].

Fuzzy inference is the process of formulating the mapping from a given input to an output using fuzzy logic. The fuzzy logic generally presents a simple knowledge of the complex and non-linear process in terms of if-then precise rules with different matching degrees for a given operational situation [37,38]. This is especially valuable where models are developed based on expert's knowledge and individuals without a mathematical background are involved. There are two kinds of fuzzy inference systems that can be implemented in the Fuzzy Logic Toolbox: Mamdani and Sugeno types.

Fuzzy logic has been increasingly used in different mineral processing fields with a variety purpose, such as crushing [39], grinding [40], flotation [4,41] and sample preparation [42] systems. Attempts to model flotation processes by a fuzzy logic approach are numerous, whether it is about models related to the entire flotation system or to specific subsystems that are its integral part.

Jahedsaravani et al. [16] used NN, adaptive neuro-fuzzy and regression methods for modeling the metallurgical factors in the batch flotation process. Their results indicated that intelligent techniques outperform statistical approaches. Carvalho and Durão [43] proposed a model based on Mamdani's fuzzy inference system within the control system for stabilizing the operation of the flotation column in a two-phase system (air and water). In another study, they more fully described the implementation of this model in the control system of a pilot flotation plant [44]. Vieira et al. [45] employed a multiple-input and multiple-output (MIMO) model to identify the performance of a flotation column using the fuzzy modeling technique, where the Takagi-Sugeno inference system was applied.

Liao et al. [46] created a fuzzy inference system within a slurry level control system in a flotation column. They considered the position of the valve that regulates the slurry level, depending on the error between the reference and measured slurry level and the change rate of that error. Jahedsaravani et al. [47] developed a fuzzy model that simulates the relationship between process conditions (air velocity, slurry solids content, frother dosage and type) and metallurgical process parameters (grade and recovery) in an industrial copper flotation column. This model was incorporated into an intelligent system for controlling the flotation process. The simulation results demonstrated that the proposed model was able to maintain the process performance at the desired values during an acceptable period of time.

Recently, Zhou and Zhou [48] proposed a fuzzy logic-based methodology for bubble edge detection in flotation froth images. Liang et al. [49] used a fuzzy logic model to optimize the configuration of flotation circuit. Gao et al. [35] applied several soft computing methodologies to develop a system that recognizes and classifies flotation froth images, including fuzzy logic.

The importance of process modeling is reflected in several technological and production aspects of flotation concentration. For example, models can be used for data analysis, which, from the aspect of the complexity of the technological process, would not be easy to achieve. Ali [50] provides several advantages that can be obtained by mathematical modeling, optimization and flotation process simulation, such as: improvement of knowledge management, better understanding of current problems, enhancement of technology transfers, decision-making support systems for plant personnel, improvements in plant work conditions, improvement in product quality, the reduction of potentially hazardous experiments, reduction of waste in process development, etc. Proper prediction of metallurgical performance factors of the flotation circuit leads to optimum production and high profit margin for industrial mineral companies.

Despite the popularity of the flotation process, and the numerous published studies, comprehensive and robust model that can represent the relationship between the operation variables (such as grinding fineness, reagent regime, slurry pH and density, residence time and similar) and performance parameters (usually concentrate quality and recovery of useful components) of the whole industrial flotation circuit is a challenging task.

Hence, finding a robust and more accurate prediction method for estimating the metallurgical performance parameters of an industrial flotation circuit is still necessary. Therefore, this work aims to assess and compare the performance of the two predictive methods that are ANN and fuzzy logic and to reveal the relevant approach for predicting the metallurgical parameters in an industrial copper flotation plant. These models are applied to a large set of industrial flotation circuit data and the results are compared in terms of accuracy, complexity and suitability for control of the flotation process. For this purpose, a real large dataset (obtained by multiannual monitoring) of the industrial copper flotation plant (Veliki Krivelj) is used. The final copper grade and recovery of the flotation circuit concentrate along with copper content in final tailings are predicted depending on the five effective variables, which are copper content in the ore feed, collector dosage in the rougher and the scavenger flotation lines, pulp pH in the rougher line and frother consumption.

The purpose of modeling the production process in Veliki Krivelj is the possibility of implementing the obtained models into an automatic control system of this process. This system would include the application of controllers based on soft computing methods, as a form of decision support for operators (fuzzy logic controller) or as an independent control unit (ANN controller). Classic PID controllers, in this case, would be used at lower hierarchical levels of control to regulate certain parameters such as: pulp level in flotation cells, air flow, pH value, value of electrochemical potential (Eh) and the like.

2. Materials and Methods

2.1. Input and Output Variables

2.1.1. Brief Description of the Veliki Krivelj Flotation Plant

The flow sheet of the Veliki Krivelj flotation circuit is shown in Figure 1. In the comminution plant, the output of three-stage crushing is fed to the two-stage grinding trains (rod mill and ball mill) in the closed circuit with cyclones to produce 58% of the product finer than 74 μm. The product of the grinding circuit is separately fed to two lines of roughing flotation cells. The first roughing flotation bank consists of 2 × 16 cells, and the second one of 3 × 21 cells. The final copper concentrate is produced by three stages of flotation cleaning. The first, second and third cleaning banks have 2 × 9, 1 × 8 and 1 × 18 cells, respectively. There is a scavenging flotation stage after the first cleaning. The scavenging bank consists of 8 cells. The combined concentrates of the roughing and scavenging lines are ground by using a regrinding mill. The tailings of the roughing and scavenging cells are discarded as the final tails. In this flotation circuit, Potassium ethyl xanthate (PEX) is used as collector and Dowfroth 250 (D-250) is used as frother. After the flotation stages, a copper concentrate was produced with an average grade and recovery of 18%–22% and 80%–90%, respectively.

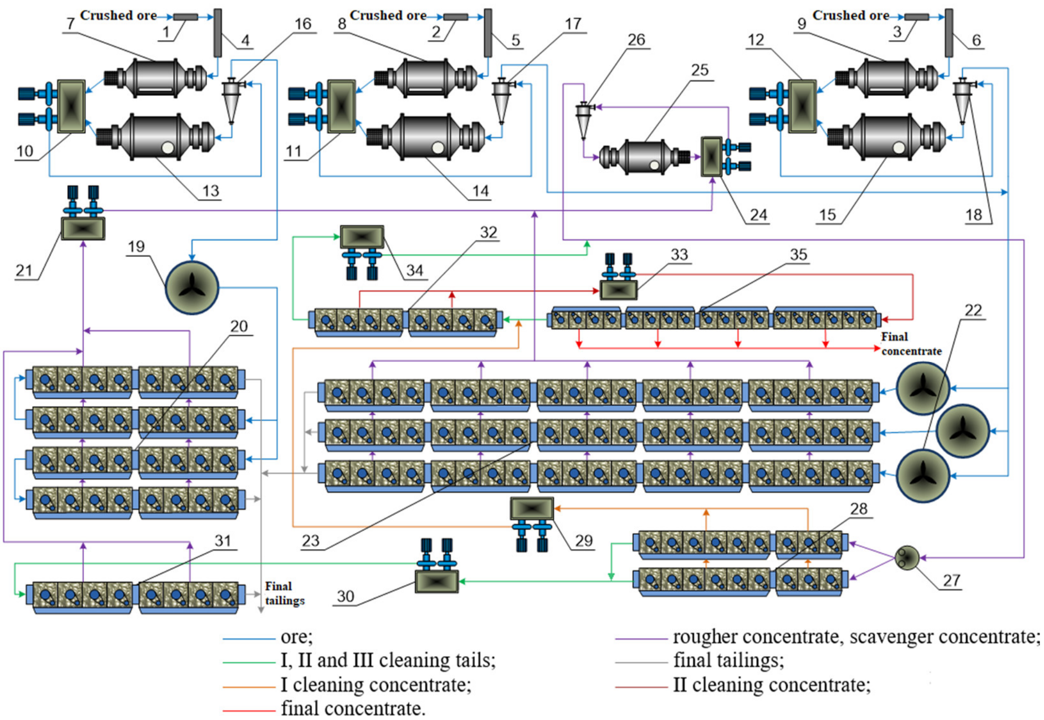

Figure 1. Process flow diagram of Veliki Krivelj flotation plant: 1–6—conveyor belts; 7–9—rod mills; 10–12, 21, 24, 29, 30, 33, 34—centrifugal slurry pumps; 13–15, 25—ball mills; 16–18, 26—hydrocyclones; 19, 22—agitators; 20, 23—roughing flotation cells; 27—divider; 28—first cleaning cells; 31—scavenging cells; 32—second cleaning cells; 35—third cleaning cells (Adapted from [4]).

2.1.2. Data Collection

The flotation process is characterized by a large number of influential parameters, i.e., input variables that influence the course of the process. All data (the input and output parameters of the model) were collected by daily/shiftly process monitoring during the multiannual plant's operation. The samples on which the copper content is determined—feed ore, final concentrate and final tailings—were taken at every hour. From the hourly increments, shift composite samples are formed (one shift lasts 8 h). On these, composites chemical analyses for copper are performed. The average consumption of reagents as well as the pulp pH value during one shift are read from the control room. More details about process parameters measurement and data collection are given in Appendix A.

Furthermore, Appendix B contains information about all datasets that were used in the process of model development and evaluation.

2.1.3. Selection of Variables

For the purposes of developing the process models, during the selection of the appropriate influential parameters, their importance was taken into account on the basis of expert analysis, as well as the availability of appropriate data. The key input variables are shown in Table 1. Other variables are considered mainly at their constant values as shown in Table 2. The output parameters of the models are shown in Table 3.

Table 1. Input (independent) parameters.

Type of Variable	Label in the Model	Unit of Measurement
Copper content in the feed	FCU	%
Collector consumption at rougher flotation circuit	PXR	g/t
Frother consumption	FRT	g/t
pH value of slurry at rougher flotation circuit	PHR	-
Collector consumption at scavenger flotation circuit	PXS	g/t

Table 2. Input variables that are considered constant.

Parameter	Value	Unit of Measurement
Grinding fineness	58	% of class −74 + 0 μm
Regrinding fineness	85	% of class −74 + 0 μm
Pulp density in rougher flotation circuit	1190	g/L
Pulp density in 1st, 2nd and 3rd cleaning	1150, 1130 and 1125	g/L
Pulp density in scavenger flotation circuit	1120	g/L
pH value in 1st, 2nd and 3rd cleaning	11.5, 11.8 and 12	-
pH value in scavenger flotation circuit	11.5	-
Residence time of rougher flotation circuit	21	minutes
Residence time of 1st, 2nd and 3rd cleaning	10, 20 and 19	minutes
Residence time of scavenger flotation circuit	10	minutes

Table 3. Output (dependent) parameters.

Type of Variable	Label in the Model	Unit of Measure
Copper content in the final concentrate	CCU	%
Copper content in the final tailings	TCU	%
Copper recovery in the final concentrate	RCU	%

The reasons for choosing constant variables are varied. For example, the liberation of the mineral raw material, i.e., its particle size distribution after grinding and regrinding is an important influencing parameter in the process. However, the analysis of the particle size distribution on the sieves is not performed daily, but as needed, every few days. The monitoring of the particle size distribution of the raw material mainly takes place on the mining pan, so there was not enough information about the changes of this parameter during each shift. Furthermore, when it comes to pulp density, there are shiftly data on the density of hydrocyclone overflows at grinding and regrinding. However, it should be taken into account that water is added to the roughing flotation cells, as well as to each cleaning stage, with the aim of correcting the pulp density. Since there is no continuous monitoring of pulp density in flotation cells, data on changes in pulp density in any of the stages of flotation concentration were not available.

By analysis of data about pH values of the hydrocyclone overflow at the regrinding, it was observed that they generally range between 9 and 10. Given that the first cleaning takes place at a pulp pH of approximately 11.5, it is clear that in the stage of the first cleaning, with addition of lime milk, was almost always necessary to achieve the desired pH value. Consequently, although there is regular monitoring and record keeping of pH values of the hydrocyclone overflow at the regrinding, these data cannot be considered confident for process model development. Choosing the consumption of the titrant in the cleaning stages as input variables makes more sense; however, from the automatic process control and regulation point of view, it is much more efficient to monitor pulp pH values (because they can be directly and continuously measured). Bearing in mind this fact, it was decided not to take the titration values into account in the modeling, but to consider the pH values of the pulp at cleaning and scavenging as constants.

It should also be noted that one of the criteria when choosing the number of input variables was the complexity of the fuzzy logic model. Specifically, when the number of input parameter increases, the number of fuzzy rules will increase exponentially [51]. This significantly increases the number of calculation and response time of fuzzy system. Therefore, the decision was to adopt an optimally small number of input parameters in the model.

In order to gain a better insight into the range and characteristics of the input and output variables, Table 4 presents some of the statistical indicators of the associated data sets.

Table 4. Statistical indicators of the input and output variables in the flotation system.

Statistical Indicator	Input Variables					Output Variables		
	FCU	PXR	FRT	PHR	PXS	CCU	TCU	RCU
Minimum	0.12	10.00	1.02	8.44	2.50	7.91	0.009	40.78
Maximum	0.51	49.98	16.97	11.97	7.90	28.09	0.149	96.48
Mean	0.26	32.27	6.19	10.40	5.38	19.24	0.041	84.24
Mod	0.26	33.50	3.80	9.85	5.00	18.48	0.035	90.77
Median	0.26	33.30	5.87	10.45	5.25	19.34	0.038	85.18
Standard deviation	0.046	5.046	2.319	0.645	0.774	3.129	0.017	6.751
Confidence interval	0.002	0.226	0.104	0.029	0.035	0.140	0.001	0.303

2.2. Methodology of Fuzzy System

Fuzzy logic is a mathematical rule-based system in which two human capabilities, which are the reasoning ability and the ability to fulfill different mental tasks, are tried to be mechanized with IF–THEN rules [52,53]. Fuzzy modeling uses linguistic expressions instead of numerical variables. The typical fuzzy logic architecture comprises four parts: 1. fuzzification, 2. fuzzy rule base, 3. fuzzy inference system (FIS) and 4. defuzzification, as it is illustrated in Figure 2 [54].

To implement a fuzzy rule-based model, the following stages are needed. First, the input and output variables are determined. Second, the fuzzy sets are determined for all variables. Within the fuzzification process, membership functions were determined for each of the input and output variable. In practice, different types of membership functions are used (such as triangular, trapezoidal, Gaussian, sigmoidal, polynominal, etc.), and the selection of the form of the membership functions will rely on the suitability of representing the element belonging to a given set and expert's decision. In this research, several membership functions—triangular, trapezoidal, Gaussian and sigmoidal right—are taken into consideration, and the most appropriate membership functions: Gaussian, trapezoidal and constant (Sugeno) were chosen. According to expert analysis, these functions gave the response surfaces most corresponding to the real process.

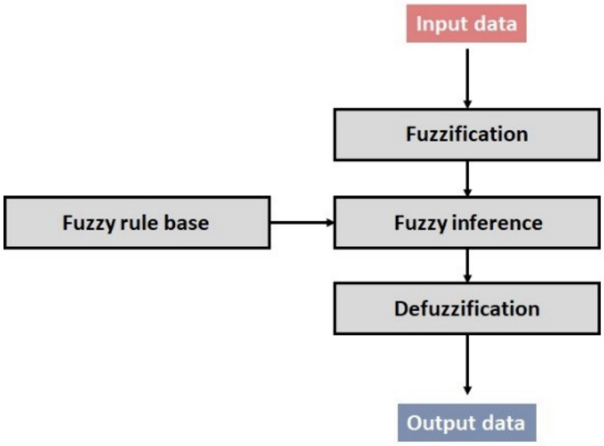

Figure 2. Fuzzy logic system [54].

FIS is the heart of the fuzzy logic system in which the classical numeric values are translated to linguistic forms. These linguistic forms are related to membership function which assigns them a membership degree (always in the interval between 0 and 1) [55]. FIS is known as a decision-making platform, which syndicates fuzzification facts with a rule base and performs the fuzzy reasoning process [56]. FIS includes membership functions, IF-THEN rules and other logical operations. IF-THEN rules are made to describe the association between input and output variables [53]. In this work, a set of the linguistic variables of a fuzzy model are specified as Low, Medium and High (see Table 5).

For the purpose of the current research, the two most common FIS types were established: the Mamdani fuzzy inference system marked as PMM and the other based on the Takagi Sugeno fuzzy inference system, marked as PSM. There are some differences between them. The PSM model is made by the appropriate transformation of the PMM model. The output of the Sugeno is linear or constant, but the output of Mamdani is the membership function. The final stage is the defuzzification in which the fuzzy results are translated to crispy form values. Some of the defuzzification techniques are the mean of the maximum, centroid, smallest of the maximum, and largest of the maximum.

In this study, the built fuzzy models are established, trained and authenticated to predict the flotation performance parameters. The input parameters are FCU, PXR, FRT, PHR, PXS, while CCU, TCU, RCU are considered as the output responses. The fuzzy models are constructed by using a fuzzy toolbox of MATLAB®. The fuzzification of the variables is performed based on the experiential knowledge of the flotation process as well as the analysis of the collected data. During the training stage, the values of the fuzzy numbers within the membership functions were adjusted. For each membership function, an appropriate type and range are determined and assigned.

In order to see more clearly the type and range of the used membership functions, in the following text, the mathematical formulas describing trapezoidal and Gaussian functions are given. Trapezoidal membership function (μ_T) is specified by four parameters (a, b, c, d) as follows:

$$\mu_T(x;a,\ b,\ c,d) = \left\{ \begin{matrix} 0,\ x \le a \\ \frac{x-a}{b-a},\ a \le x \le b \\ 1,\ b \le x \le c \\ \frac{d-x}{d-c},\ c \le x \le d \\ 0,\ d \le x \end{matrix} \right\} \tag{1}$$

where the parameters a, b, c and d (with $a < b \le c < d$) determine the x coordinates of the four corners of the underlying trapezoidal membership function. An illustration of this membership function is given in Figure 3a.

Table 5. Fuzzification of the range of variables in the PMM and PSM.

Variable		Membership Function	Range of Values	Range Fuzzification (Linguistic Value of the Variable)
Input (independent)	FCU	Gaussian	σ/2 = 0.04778; c = 0.112 σ/2 = 0.07976; c = 0.3008 σ/2 = 0.02871; c = 0.492	Low Medium High
	PXR	Gaussian	σ/2 = 4.743; c = 10.5 σ/2 = 6.37; c = 30.0 σ/2 = 4.678; c = 49.0	Low Medium High
	FRT	Gaussian	σ/2 = 1.362; c = 0.325 σ/2 = 1.486; c = 6.5 σ/2 = 5.335; c = 17.4	Low Medium High
	PHR	Gaussian	σ/2 = 0.779; c = 8.08 σ/2 = 0.598; c = 9.989 σ/2 = 1.071; c = 11.88	Low Medium High
	PXS	Gaussian	σ/2 = 1.225; c = 2.2 σ/2 = 0.7887; c = 6.0 σ/2 = 0.3802; c = 7.9	Low Medium High
Output PMM	CCU	Trapezoidal	a = 3.439; b = 6.845; c = 8.015; d = 13.98 a = 10.16; b = 12.36; c = 15.28; d = 21.66 a = 19.78; b = 24.18; c = 25.38; d = 28.08	Low Medium High
	RCU	Trapezoidal	a = 34.32; b = 43.92; c = 54.12; d = 65.73 a = 56.05; b = 71.45; c = 76.15; d = 94.35 a = 61.90; b = 82.32; c = 89.90; d = 100.0	Low Medium High
	TCU	Trapezoidal	a = 0.0124; b = 0.0394; c = 0.0461; d = 0.0731 a = 0.0609; b = 0.0878; c = 0.0946; d = 0.1216 a = 0.1227; b = 0.1497; c = 0.1565; d = 0.1834	Low Medium High
Output PSM	CCU	Constant	z = 8.8 z = 15.08 z = 24.25	Low Medium High
	RCU	Constant	z = 49.61 z = 74.69 z = 83.07	Low Medium High
	TCU	Constant	z = 0.0427 z = 0.0912 z = 0.153	Low Medium High

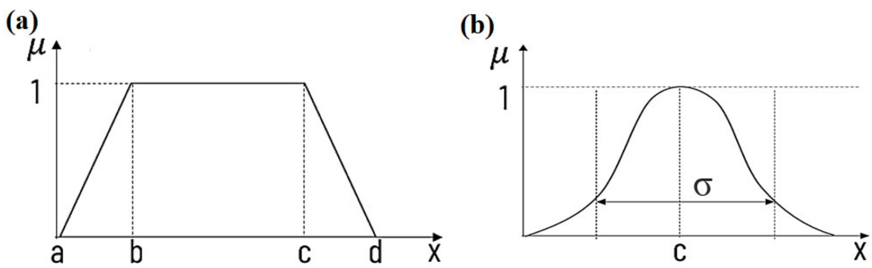

Figure 3. Membership functions: (**a**) Trapezoidal; (**b**) Gaussian.

Gaussian membership function (μ_G) is specified by two parameters (c, σ) as follows:

$$\mu_G(x; c, \sigma) = e^{-\frac{1}{2}\left(\frac{x-c}{\sigma}\right)^2} \tag{2}$$

where c represents the membership functions center and σ determines the membership function width. An illustration is given in Figure 3b.

Table 5 shows the fuzzified linguistic values of the input and output variables. The parameter labels given in the column entitled "Range of values" correspond to those in Equations (1) and (2). Figures 4 and 5 show the examples of defined membership functions.

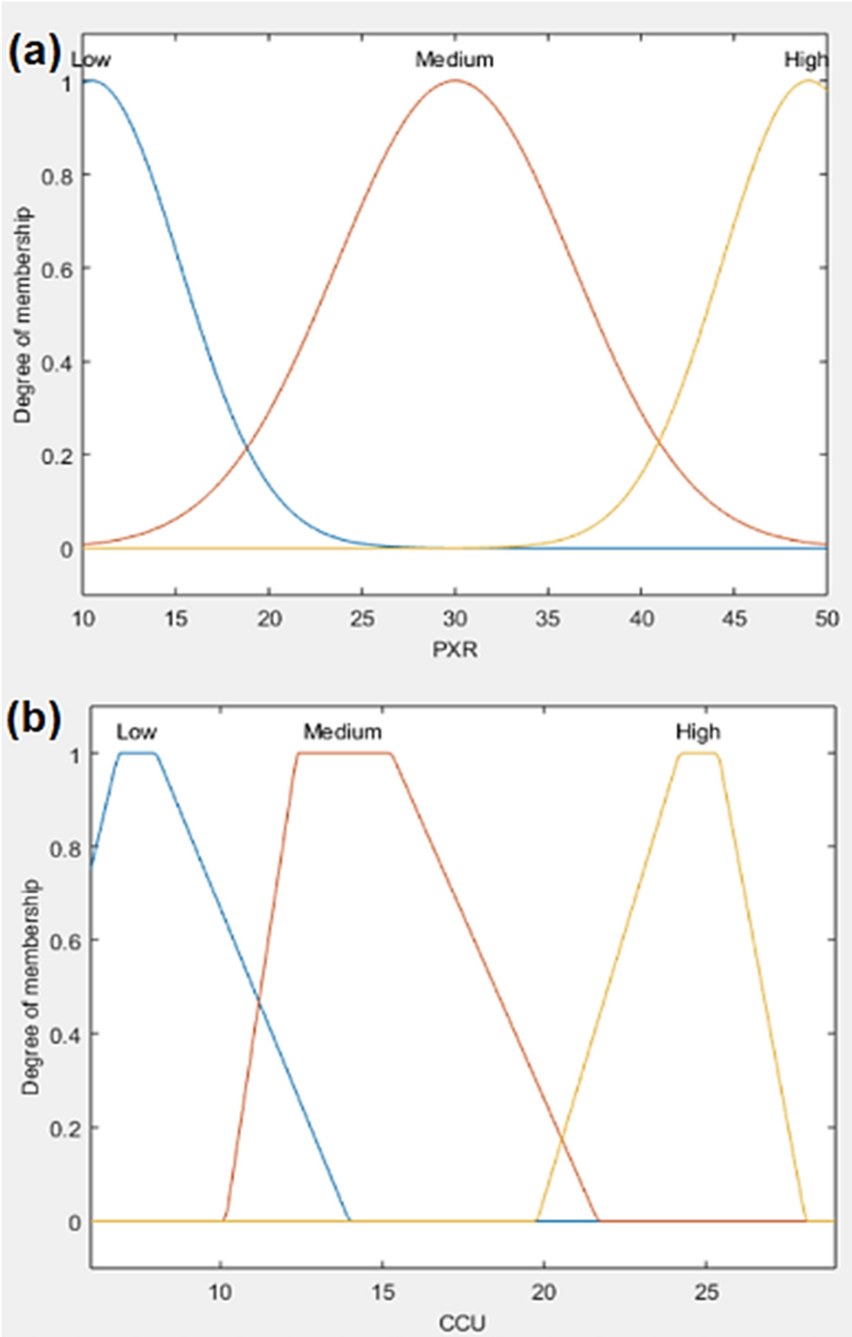

Figure 4. Example of defining the parameters of membership functions in the PMM: (**a**) collector consumption at rougher flotation circuit (PXR); (**b**) copper content in final concentrate (CCU).

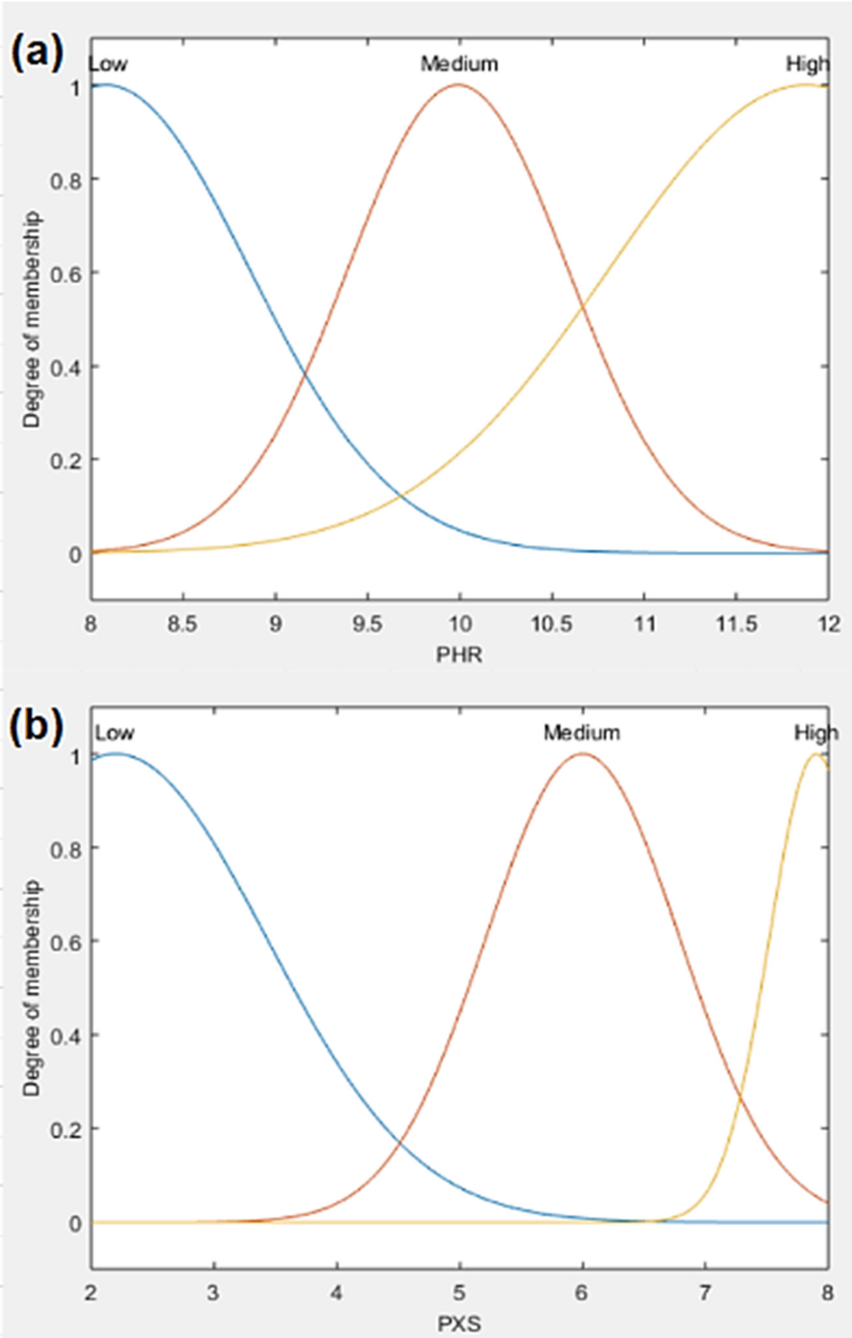

Figure 5. Example of defining the parameters of membership functions in the PSM: (**a**) pH value at rougher flotation circuit (PHR); (**b**) collector consumption in scavenging circuit (PXS).

As a starting point for defining fuzzy rules, Table 6 shows the interdependence matrix of process parameters of the flotation process. The action, that is, the behavior of dependent variables in the process, was considered for the case of an increase in the value of independent variable factors (understood within the established range, with no influence of the remained parameters).

By combining the linguistic values of the input and output variables using the logical operators of conjunction (AND) or disjunction (OR), fuzzy rules of the following type were formed (Table 7):

Fuzzy rules were formed based on literature review and expert knowledge of the flotation process. In this process, 753 rules were constructed by using a rule editor in a fuzzy toolbox environment. Figure 6 shows the details of rule bases for PMM and PSM models, where the rule constituents are expressed through membership functions. This display of the rule base allows the possibility of setting the values of the input parameters and insight into the resulting values of the output variables.

Table 6. Interdependence matrix of parameters in the flotation process.

Independent Variable	Action [1]		
	CCU	RCU	TCU
FCU	↑	↓	↑
PXR	↑	↑	↓
FRT	↓	↑	↓
PHR	↑	↓	↑
PXS	↓	↑	↓

[1] ↑—increase; ↓—decrease.

Table 7. Fuzzy rules formation.

IF FCU is "*low*" **AND** PXR is "*high*" **AND** FRT is "*medium*" **AND** PHR is "*medium*" **AND** PXS is "*high*"
THEN CCU is "*medium*" **AND** TCU is "*low*" **AND** RCU is "*high*"
IF FCU is "*medium*" **AND** PXR is "*medium*" **AND** FRT is "*high*" **AND** PHR is "*low*" **AND** PXS is "*medium*"
THEN CCU is "*medium*" **AND** TCU is "*medium*" **AND** RCU is "*high*"
IF FCU is "*high*" **AND** PXR is "*medium*" **AND** FRT is "*medium*" **AND** PHR is "*high*" **AND** PXS is "*low*"
THEN CCU is "*high*" **AND** TCU is "*medium*" **AND** RCU is "*medium*"
⋮
etc.

2.2.1. Fuzzy Logic Model Based on Mamdani Inference System—PMM

The elementary characteristics of the PMM model are as following:

- Mamdani inference system;
- Applied AND operator in all rules;
- Implication by the minimum method;
- Aggregation by the maximum method; and
- Defuzzification by the centroid method.

PMM model contains a base of 753 rules. The resulting surfaces are shown in Figures 7–9.

By observing the obtained surfaces, and taking into account predefined boundaries, it can generally be concluded that these surfaces follow real dependencies of the process parameters to an acceptable extent. Due to the existence of a large number of resulting surfaces, a detailed analysis of each surface would require a too extensive textual presentation. Therefore, the authors decided to analyze two resulting surfaces of the PMM model:

(1) The surface that shows the dependence of the final concentrate grade (CCU) on copper content in the feed (FCU) and collector consumption at a rougher flotation circuit (PXR), Figure 7c;
(2) The surface that demonstrates dependence of the final grade of tailings (TCU) on the copper content in the feed (FCU) and frother consumption (FRT), Figure 9a.

By visual analysis of the first chosen surface, Figure 7c, it can be observed that with increasing the collector dosage to a certain extent, the copper grade of the final concentrate increases and then decreases with a further increase in collector dosage. Similarly, with increasing the copper content in the feed ore, the quality of the final concentrate also increases. When we consider the second chosen surface, Figure 9a, it can be observed that an increase in the frother dosage leads to the reduction of the copper content in the tailings. These characteristics are in alignment with the literature [57–59].

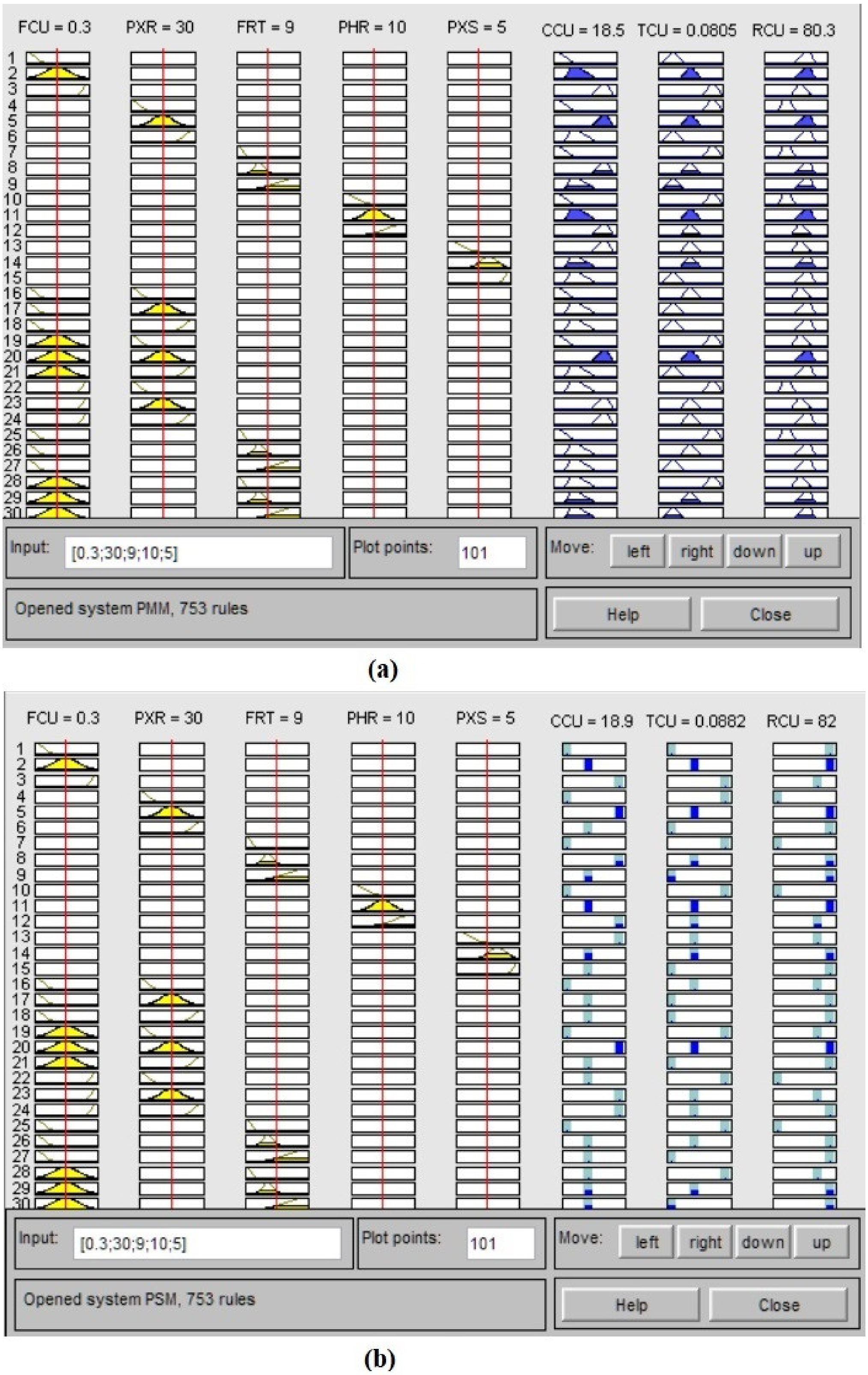

Figure 6. Display of the detail of the rule base: (**a**) PMM and (**b**) PSM model.

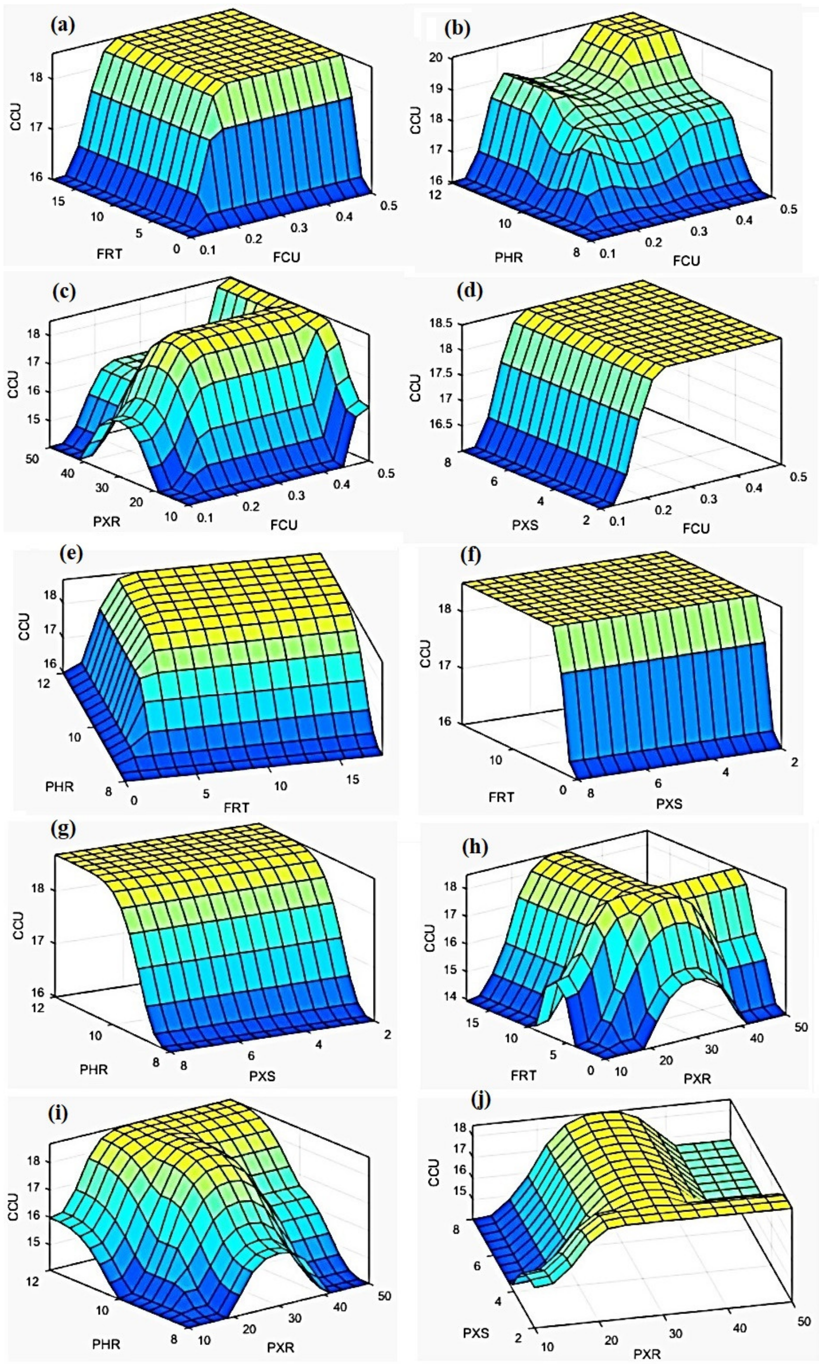

Figure 7. Resulting response surfaces of the PMM model—dependence of final concentrate quality (CCU) on input parameters. (**a**) copper content in the feed (FCU) and frother consumption (FRT); (**b**) copper content in the feed (FCU) and pH value of slurry at rougher flotation circuit (PHR); (**c**) copper content in the feed (FCU) and collector consumption at rougher flotation circuit (PXR); (**d**) copper content in the feed (FCU) and collector consumption at scavenger flotation ciruit (PXS); (**e**) frother consumption (FRT) and pH value of slurry at rougher flotation circuit (PHR); (**f**) frother consumption (FRT) and collector consumption at scavenger flotation ciruit (PXS); (**g**) pH value of slurry at rougher flotation circuit (PHR) and collector consumption at scavenger flotation ciruit (PXS); (**h**) frother consumption (FRT) and collector consumption at rougher flotation circuit (PXR); (**i**) pH value of slurry at rougher flotation circuit (PHR) and collector consumption at rougher flotation circuit (PXR); (**j**) collector consumption at scavenger flotation ciruit (PXS) and collector consumption at rougher flotation circuit (PXR).

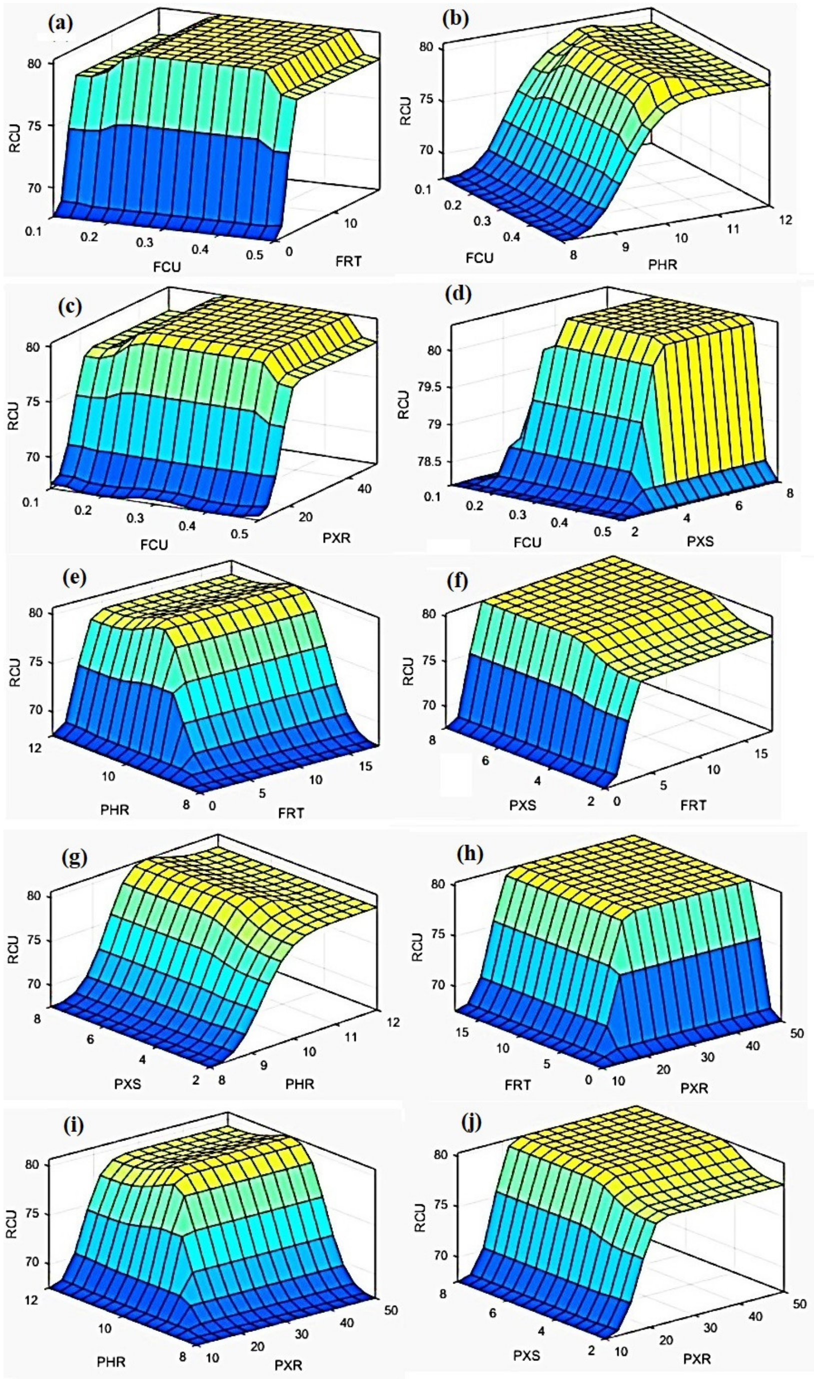

Figure 8. Resulting response surfaces of the PMM model—dependence of copper recovery in final concentrate (RCU) on input parameters. (**a**) copper content in the feed (FCU) and frother consumption (FRT); (**b**) copper content in the feed (FCU) and pH value of slurry at rougher flotation circuit (PHR); (**c**) copper content in the feed (FCU) and collector consumption at rougher flotation circuit (PXR); (**d**) copper content in the feed (FCU) and collector consumption at scavenger flotation ciruit (PXS); (**e**) frother consumption (FRT) and pH value of slurry at rougher flotation circuit (PHR); (**f**) frother consumption (FRT) and collector consumption at scavenger flotation ciruit (PXS); (**g**) pH value of slurry at rougher flotation circuit (PHR) and collector consumption at scavenger flotation ciruit (PXS); (**h**) frother consumption (FRT) and collector consumption at rougher flotation circuit (PXR); (**i**) pH value of slurry at rougher flotation circuit (PHR) and collector consumption at rougher flotation circuit (PXR); (**j**) collector consumption at scavenger flotation ciruit (PXS) and collector consumption at rougher flotation circuit (PXR).

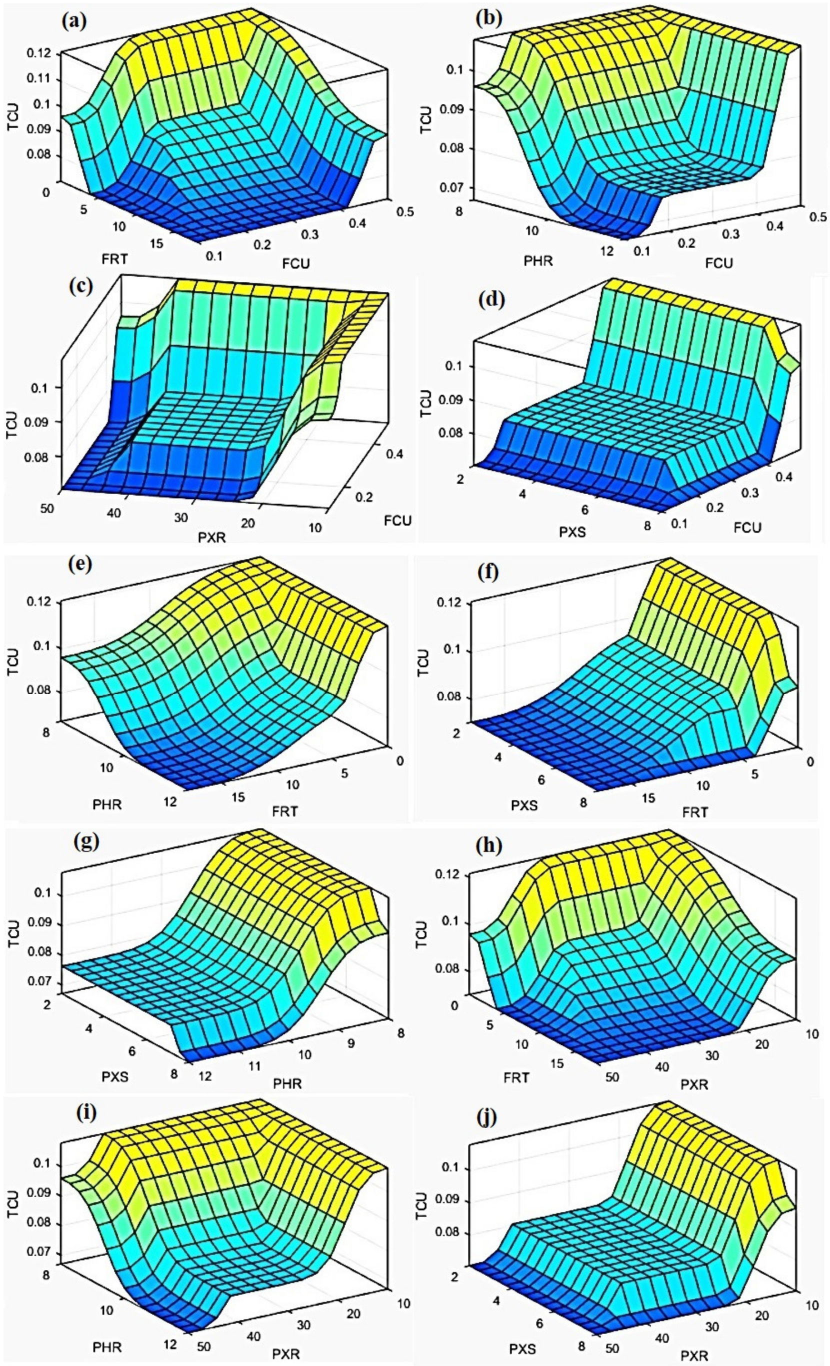

Figure 9. Resulting response surfaces of the PMM model—dependence of copper content in final tailings (TCU) on input parameters. (**a**) copper content in the feed (FCU) and frother consumption (FRT); (**b**) copper content in the feed (FCU) and pH value of slurry at rougher flotation circuit (PHR); (**c**) copper content in the feed (FCU) and collector consumption at rougher flotation circuit (PXR); (**d**) copper content in the feed (FCU) and collector consumption at scavenger flotation ciruit (PXS); (**e**) frother consumption (FRT) and pH value of slurry at rougher flotation circuit (PHR); (**f**) frother consumption (FRT) and collector consumption at scavenger flotation ciruit (PXS); (**g**) pH value of slurry at rougher flotation circuit (PHR) and collector consumption at scavenger flotation ciruit (PXS); (**h**) frother consumption (FRT) and collector consumption at rougher flotation circuit (PXR); (**i**) pH value of slurry at rougher flotation circuit (PHR) and collector consumption at rougher flotation circuit (PXR); (**j**) collector consumption at scavenger flotation ciruit (PXS) and collector consumption at rougher flotation circuit (PXR).

2.2.2. Fuzzy Logic Model Based on Takagi Sugeno Inference System—PSM

The fuzzy logic model was formed by applying a suitable transformation of the PSM model. Its basic methodological characteristics are as follows:

- Takagi-Sugeno inference system; applied AND operator in all rules;
- Implication by the product method;
- Aggregation by the sum method and
- Defuzzification by the weighted average method.

The surfaces obtained by the Takagi Sugeno methodology were smoother than those obtained by the Mamdani fuzzy inference system, which is expected [60]. In general, it can be concluded that these surfaces follow the real dependencies of the process parameters somewhat better than the PMM model. As in the previous section, a detailed analysis of all surfaces requires a substantial textual representation. Because of that, the analyses of two selected resulting surfaces are given in this section:

(1) The surface that shows the dependence of the final concentrate grade (CCU) on the copper content in the feed (FCU) and the pulp pH at the rougher circuit (PHR), Figure 10b; and
(2) The surface that displays the dependence of copper recovery in the final concentrate (RCU) on the copper content in the feed (FCU) and the consumption of the collector at the scavenger circuit (PXS), Figure 11d.

It is known from practice that an increase in the pulp pH leads to an increase in the copper grade of concentrate, which can also be observed from the first selected surface, Figure 10b. At first glance, the question of the regularity of the given surface can be imposed, considering that in this case only the pH value at the rough flotation is considered. However, we should not ignore the fact that the pH values in the other stages of flotation are considered optimal constants, and therefore this surface is justified from the aspect of the flotation concentration process as a whole.

The main reason for adding the collector at the scavenger stage is to increase the recovery of copper in the concentrate, which coincides with the appearance of the second selected surface, Figure 11d.

In industrial conditions, the increase in the copper content in the feed ore increase the concentrate grade. Moreover, if the feed is poor, recovery increases to a certain extent, and with a further increase in Cu in the feed, recovery decreases, because a part of the copper remains in the tailings. These technological actualities correspond to both observed surfaces.

2.3. Artificial Neural Network

NNs are used for solving complex and nonlinear engineering problems. NNs is a widely used model in mineral processing applications with the ability to recognize patterns among parameters and predict the key performance parameters of the processes. A typical NN comprises a large number of neurons or nodes, which are connected to each other. The neurons are grouped in layers and connected by weighted links and bias. The output of each neuron is transferred to the next layer as an input. Finally, the nonlinear basis function set is used to calculate the outputs of NN. The model learning is modifying the weights and biases to minimize the error, taking into account the targets. Details of the NN algorithm procedure are presented by Nakhaei et al. [61,62].

In the current study, three feed-forward back-propagation learning algorithms were employed for predicting the copper content in the final concentrate (NN1), copper recovery in the final concentrate (NN2), and copper content in the final tailings (NN3). A simple architecture for the model structures established in this study is shown in Figure 13.

The base also contains 753 rules, as well as the corresponding Mamdani model. The resulting surfaces of the PSM model are presented in Figures 10–12.

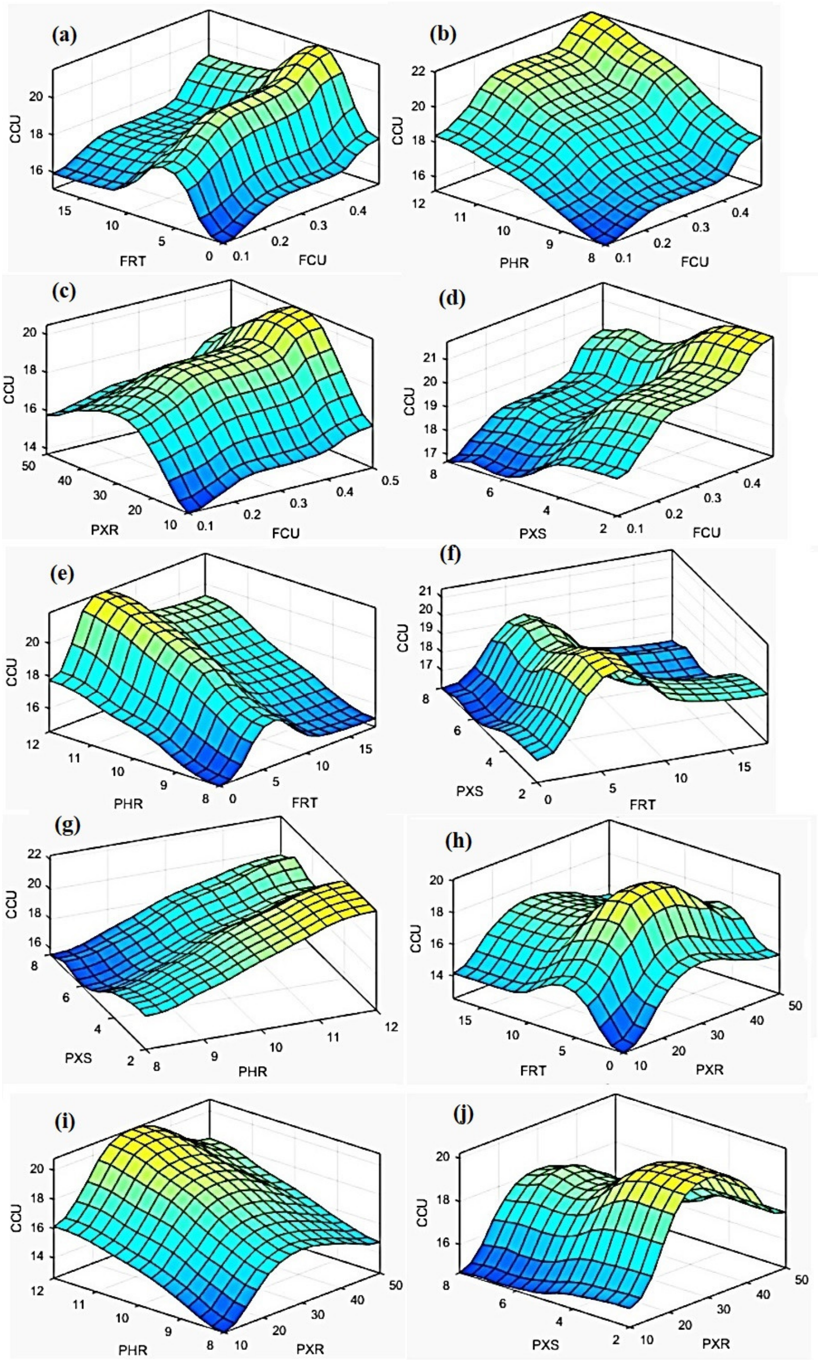

Figure 10. Resulting response surfaces of the PSM model—dependence of final concentrate quality (CCU) on input parameters. (**a**) copper content in the feed (FCU) and frother consumption (FRT); (**b**) copper content in the feed (FCU) and pH value of slurry at rougher flotation circuit (PHR); (**c**) copper content in the feed (FCU) and collector consumption at rougher flotation circuit (PXR); (**d**) copper content in the feed (FCU) and collector consumption at scavenger flotation ciruit (PXS); (**e**) frother consumption (FRT) and pH value of slurry at rougher flotation circuit (PHR); (**f**) frother consumption (FRT) and collector consumption at scavenger flotation ciruit (PXS); (**g**) pH value of slurry at rougher flotation circuit (PHR) and collector consumption at scavenger flotation ciruit (PXS); (**h**) frother consumption (FRT) and collector consumption at rougher flotation circuit (PXR); (**i**) pH value of slurry at rougher flotation circuit (PHR) and collector consumption at rougher flotation circuit (PXR); (**j**) collector consumption at scavenger flotation ciruit (PXS) and collector consumption at rougher flotation circuit (PXR).

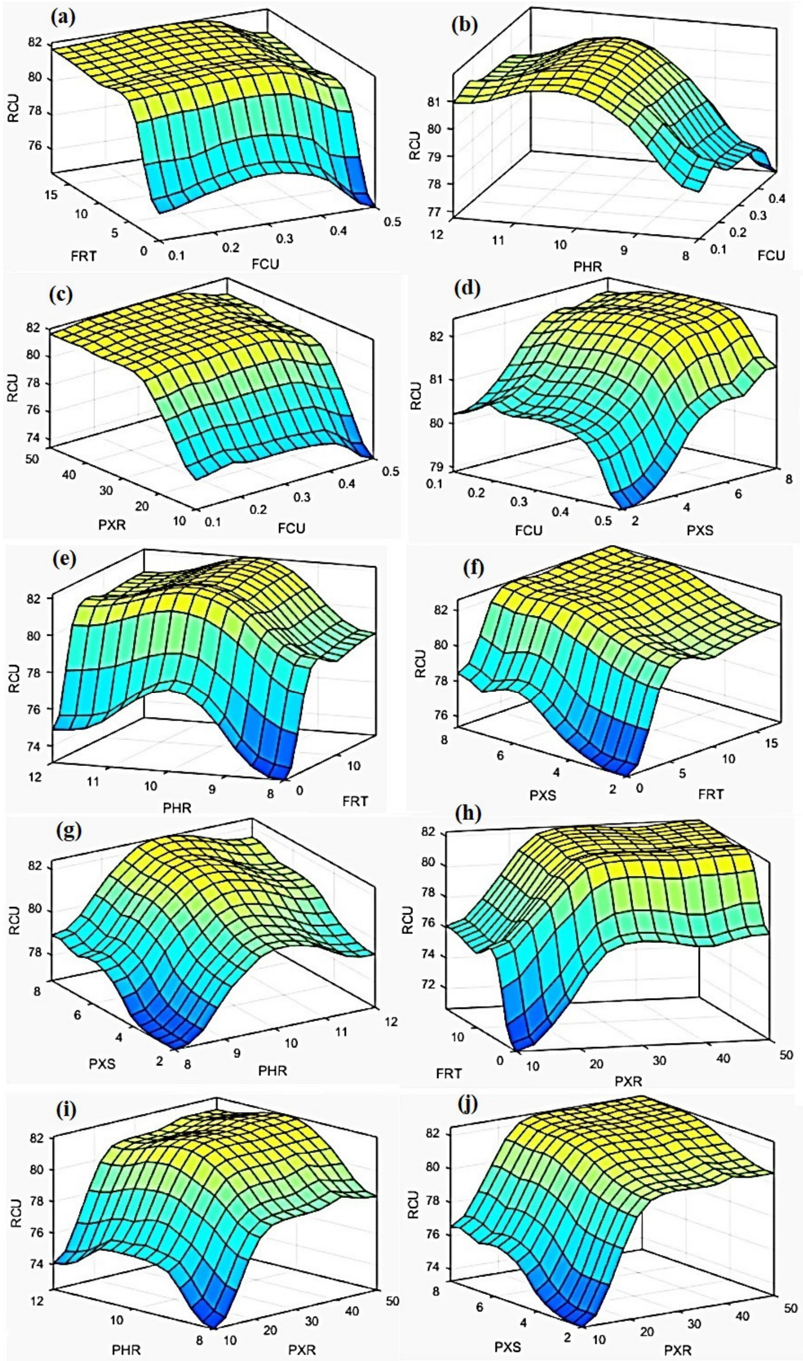

Figure 11. Resulting response surfaces of the PSM model—dependence of copper recovery (RCU) in final concentrate on input parameters. (**a**) copper content in the feed (FCU) and frother consumption (FRT); (**b**) copper content in the feed (FCU) and pH value of slurry at rougher flotation circuit (PHR); (**c**) copper content in the feed (FCU) and collector consumption at rougher flotation circuit (PXR); (**d**) copper content in the feed (FCU) and collector consumption at scavenger flotation ciruit (PXS); (**e**) frother consumption (FRT) and pH value of slurry at rougher flotation circuit (PHR); (**f**) frother consumption (FRT) and collector consumption at scavenger flotation ciruit (PXS); (**g**) pH value of slurry at rougher flotation circuit (PHR) and collector consumption at scavenger flotation ciruit (PXS); (**h**) frother consumption (FRT) and collector consumption at rougher flotation circuit (PXR); (**i**) pH value of slurry at rougher flotation circuit (PHR) and collector consumption at rougher flotation circuit (PXR); (**j**) collector consumption at scavenger flotation ciruit (PXS) and collector consumption at rougher flotation circuit (PXR).

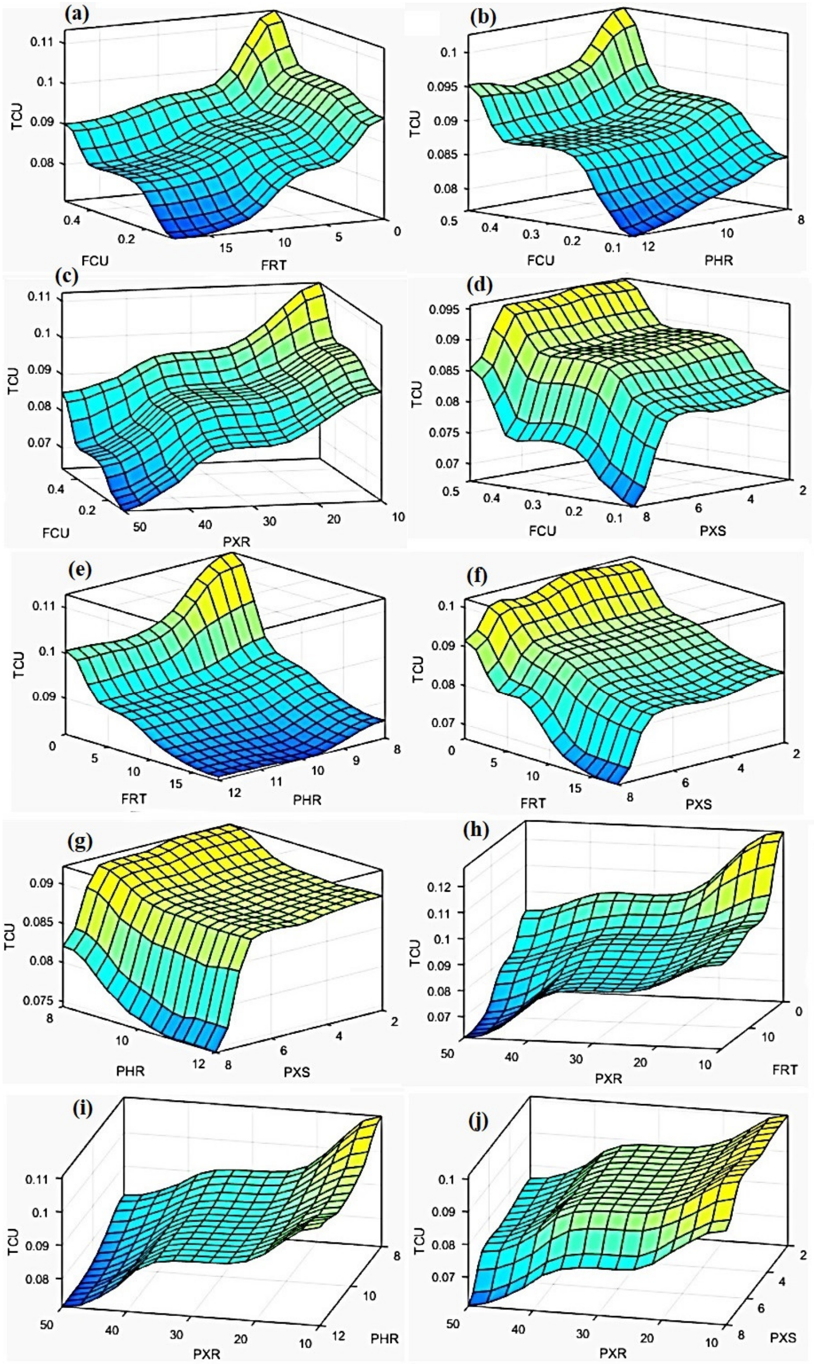

Figure 12. Resulting response surfaces of the PSM model—dependence of copper content in final tailings (TCU) on input parameters. (**a**) copper content in the feed (FCU) and frother consumption (FRT); (**b**) copper content in the feed (FCU) and pH value of slurry at rougher flotation circuit (PHR); (**c**) copper content in the feed (FCU) and collector consumption at rougher flotation circuit (PXR); (**d**) copper content in the feed (FCU) and collector consumption at scavenger flotation ciruit (PXS); (**e**) frother consumption (FRT) and pH value of slurry at rougher flotation circuit (PHR); (**f**) frother consumption (FRT) and collector consumption at scavenger flotation ciruit (PXS); (**g**) pH value of slurry at rougher flotation circuit (PHR) and collector consumption at scavenger flotation ciruit (PXS); (**h**) frother consumption (FRT) and collector consumption at rougher flotation circuit (PXR); (**i**) pH value of slurry at rougher flotation circuit (PHR) and collector consumption at rougher flotation circuit (PXR); (**j**) collector consumption at scavenger flotation ciruit (PXS) and collector consumption at rougher flotation circuit (PXR).

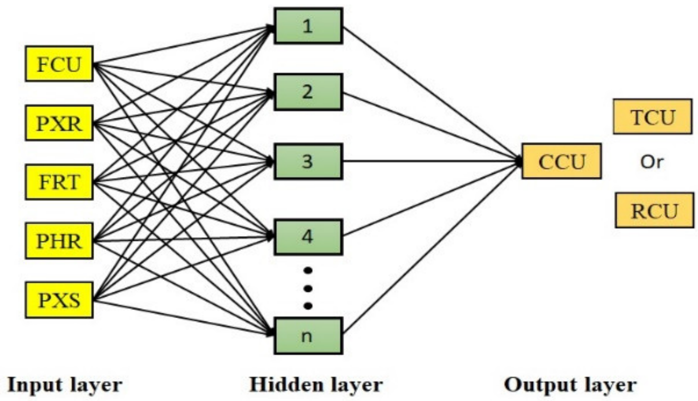

Figure 13. The structure of the NN models for the prediction of CCU, RCU and TCU from the industrial flotation plant.

The ANN models consist of one input layer with five elements (FCU, PXR, FRT, PHR and PXS), one hidden layer including the desired number of nodes, and the output layer where the CCU, RCU and TCU values are calculated. The logsigmoid and purelin functions (see Figure 14) are implemented as the activation functions in the hidden layer and the output layer. The optimum NN structure is selected using the "trial and error" method by adjusting the number of neurons in the hidden layer (from 10 to 100) in order to achieve the best model by minimizing the errors. The widely applied Levenberg Marquardt (LM) algorithm is used for the model training. For the purposes of designing the network, 1910 data were selected.

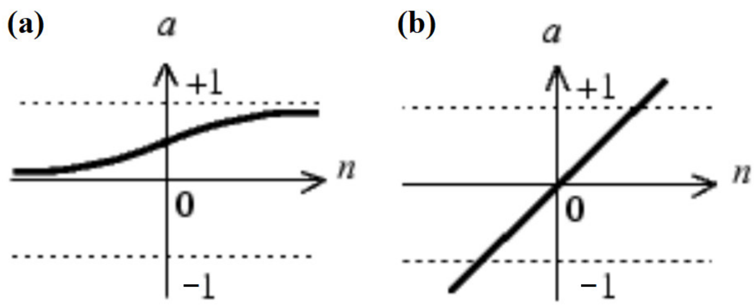

$$a = logsig(n) = \frac{1}{1 + e^{-n}} \qquad a = purelin(n) = n$$

Figure 14. Activation functions: (**a**) logsigmoid; (**b**) purelin.

The first idea was to develop one ANN model consisting of 5 input and 3 output variables. However, the selected software tool considers the sets of output data as one set and performs all calculations and interpretations based on it. Since the output parameters are numerically independent and expressed in different units, this was not acceptable. Moreover, ANN models were developed in order to compare their performances with performances of fuzzy logic models. Given that fuzzy logic models were developed based on original data (without normalization), the same procedure was applied to neural networks. The building of new ANN models with 3 output variables, using more advanced software tools and normalized data sets, is a topic for further research.

3. Results and Discussion

3.1. Performance Evaluation of the Fuzzy Models

The evaluation of the proposed models was carried out in the MATLAB software package, by entering the real values of the input process variables from the industrial flotation plant "Veliki Krivelj" and generating the corresponding outputs predicted by the models. Several standard statistical criteria, including the determination coefficient (R^2), root mean square error (RMSE), and standard deviation of prediction error (SDE), are used to evaluate the performance of the developed models. R^2 is an indicator of how much changes in one variable are caused by changes in another variable, and is represented by Equation (3), while *RMSE* shows the accuracy of the model's predicted values versus the actual, and is represented by Equation (4):

$$R^2 = \left[\frac{n(\sum XY) - (\sum X)(\sum Y)}{\sqrt{\left(n \sum X^2 - (\sum X)^2\right)\left(n \sum Y^2 - (\sum Y)^2\right)}} \right]^2 \tag{3}$$

$$RMSE = \sqrt{\frac{\sum_{i=1}^{n} (X - Y)^2}{n}} \tag{4}$$

In these equations, X is the measured value, Y is the predicted value, and n is the number of samples.

SDE shows how much, on average, the elements of the dataset deviate from the arithmetic mean of that dataset and is expressed by Formula (5):

$$SDE = \sqrt{\frac{\sum_{i=1}^{n} (x - \mu)^2}{n}} \tag{5}$$

where n presents the number of elements in the dataset, μ is mean (average value) of the dataset and x is the i-th member of the dataset.

Standard deviation is determined for absolute (SDE) and relative prediction error (SDE_r).

The prediction error (ε) and relative prediction error (ε_r), which served as the criteria for evaluating the predictive properties of models, were calculated according to the Formulas (6) and (7):

$$\varepsilon = Y - X \tag{6}$$

$$\varepsilon_r = \frac{Y - X}{X} \tag{7}$$

where X, Y have the same meaning as in Equations (3) and (4).

The descriptive statistics of differences between measured and estimated values for the evaluation data are given in Tables 8 and 9. Figures 15–18 present the prediction errors of the fuzzy models.

Table 8. Statistical analysis of actual and predicted values using the PMM model.

Statistical Parameters	Technological Indicator of the Flotation Process		
	CCU	**RCU**	**TCU**
R^2	0.971	0.992	0.839
RMSE	3.126	7.007	0.034
Mean of prediction error, μ	−0.886	−2.666	0.044
SDE	3.306	7.227	0.019
Maximum positive error (maximum)	10.644	36.739	0.100
Minimum positive error	0.00069	0.00689	0.00015
Minimum negative error	−0.01968	−0.01318	−0.00001
Maximum negative error (minimum)	−10.743	−25.233	−0.047
Mean of relative prediction error, μ_r	−0.017	−0.024	1.485
SDE_r	0.190	0.098	1.238

Table 9. Statistical analysis of actual and predicted values using the PSM model.

Statistical Parameters	Technological Indicator of the Flotation Process		
	CCU	RCU	TCU
R^2	0.970	0.993	0.847
RMSE	3.291	6.739	0.034
Mean of prediction error	−0.288	−2.008	0.046
SDE	3.374	6.915	0.018
Maximum positive error (maximum)	10.961	39.619	0.091
Minimum positive error	0.00473	0.00232	0.00128
Minimum negative error	−0.01028	−0.01190	−0.00019
Maximum negative error (minimum)	−10.354	−17.502	−0.056
Mean of relative prediction error, μ_r	0.015	−0.0165	1.562
SDE_r	0.198	0.096	1.244

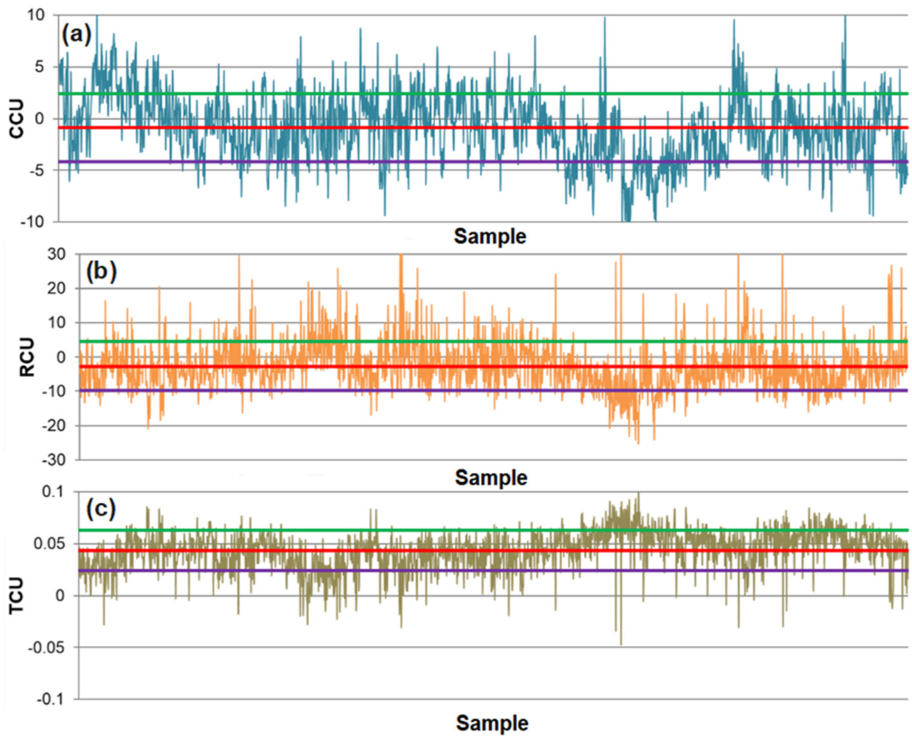

Figure 15. Prediction errors of technological indicators according to the PMM model: (**a**) CCU, (**b**) RCU and (**c**) TCU. The red line on the charts represents mean (μ), green line value μ + 1 SDE and purple line value μ − 1 SDE.

By considering the results of the regression analysis shown in Table 8, it can be observed that the values of the determination coefficients for predictions of the content and recovery of copper in the final concentrate are high. This means that a strong relationship has been established using the PMM model between the actual and the predicted values of the metallurgical indicators. In other words, the proposed model well describes the changes in the real values of the observed parameters related to their increase or decrease over time.

Yet, when the prediction error is taken into account (Figure 15), it is noted that there are insignificant and, in some occasions, relatively large deviations from the actual results. Although the maximum and minimum errors of the estimation (margin of error) are high, they occurred a few times and did not have a high frequency.

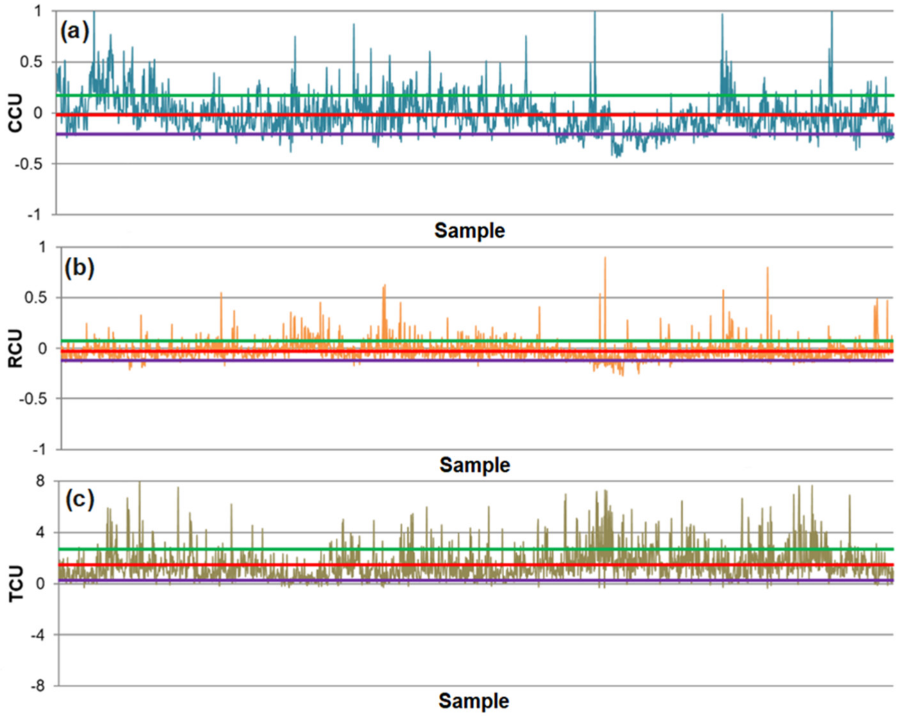

Figure 16. Relative prediction errors of technological indicators according to the PMM model: (**a**) CCU, (**b**) RCU and (**c**) TCU. The red line on the charts represents mean (μ_r), green line value μ_r + 1 SDE_r and violet line value $\mu_r - 1$ SDE_r.

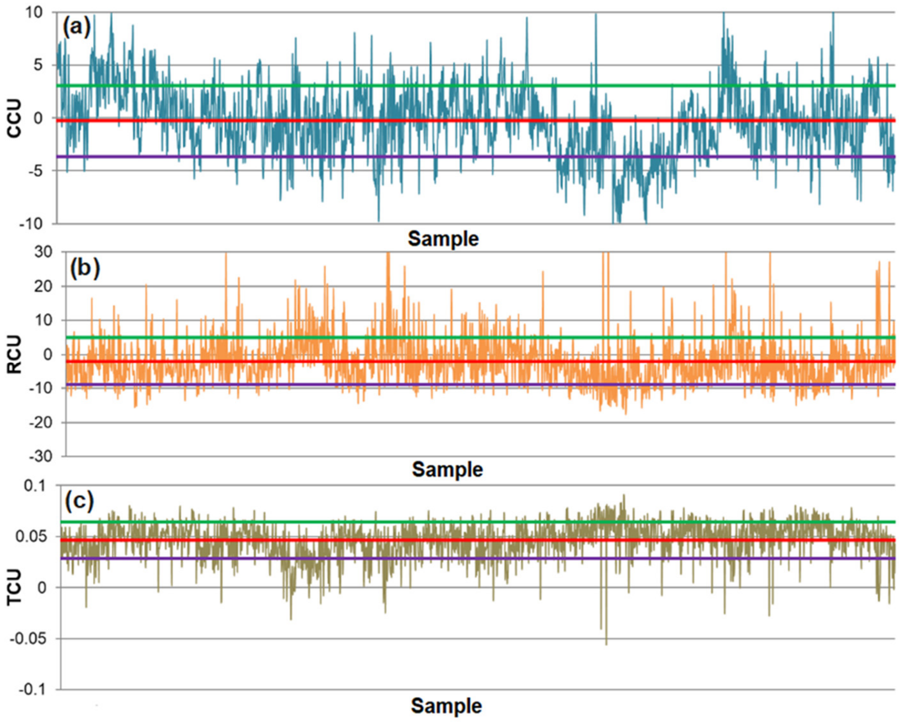

Figure 17. Prediction errors of technological indicators according to the PSM model: (**a**) CCU, (**b**) RCU and (**c**) TCU. The red line on the charts represents mean (μ), green line value μ + 1 SDE and purple line value $\mu - 1$ SDE.

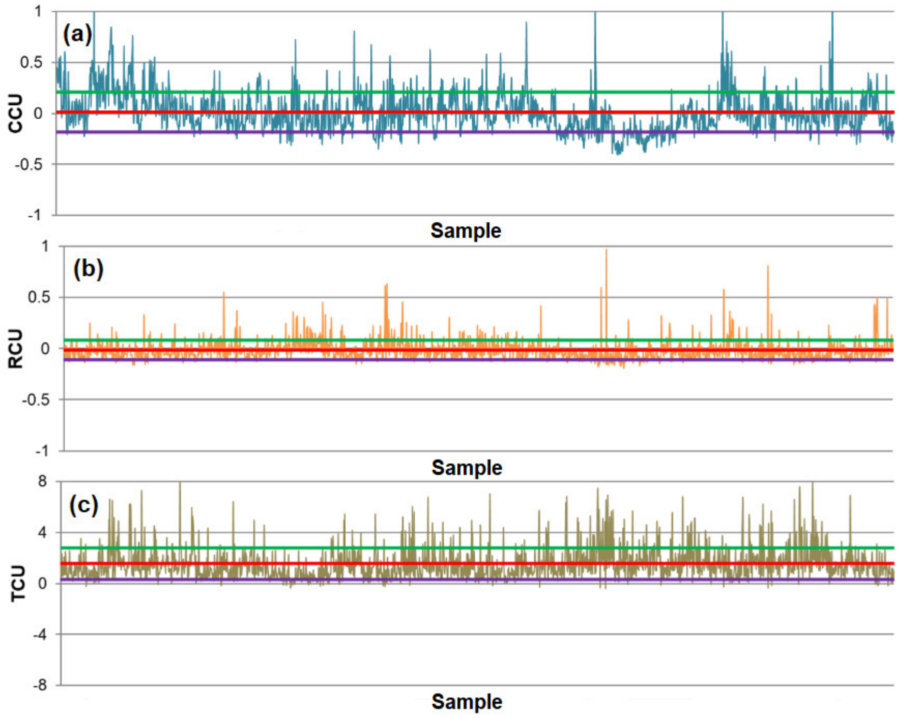

Figure 18. Relative prediction errors of technological indicators according to the PSM model: (**a**) CCU, (**b**) RCU and (**c**) TCU. The red line on the charts represents mean (μ_r), green line value μ_r + 1 SDE_r and violet line value $\mu_r - 1$ SDE_r.

The red line on the charts represents mean (μ), green line value μ + 1 SDE and purple line value μ − 1 SDE. This is generally applied to all charts where absolute and relative prediction error is presented.

It should be noted that the complete regression analysis was based on a theoretical assumption that if the actual values of the metallurgical indicators were equal to zero, in that case the values predicted by the models would also be equal to zero. This statement was adopted for practical reasons, in order to mitigate illogical oscillations, extreme deviations and dispersion of values in real results, caused by imperfections in measurement, human factor errors and the like, which can significantly affect the results of the model validation. In this sense, this regression analysis should be given greater mathematical importance than the practical.

By observing the trend of the prediction errors of the final concentrate grade, it can be concluded that their values are mostly between ± 5% Cu, which is consistent with the RMSE value of 3.126 (Table 8). The only major deviation from this trend can be observed on the right half of the diagram, which corresponds to the beginning of the last third of the observed time period of the plant operation. In this period, prediction errors are mostly negative, which may indicate changes in the operation conditions of the plant. These large fluctuations can be caused by changing some factors that were not taken into account during modeling, such as changes in the feed ore hardness or changes in the quality of the reagents.

Furthermore, by looking at the prediction errors of recovery, it is observed that a positive prediction error for the recovery (predicted values are higher than the actual) is quite well associated to a negative prediction error for the tailings grade. The reverse is also true: a negative prediction error for the recovery is associated to a positive prediction error for the tailings grade. Therefore, the recovery of copper in the final concentrate and the copper content in the tailings are in alignment with each other. This matching indicates a good general setting of the model, as well as the potential influence of process factors that were considered constant during modeling.

It should also be noted that the TCU prediction error is mostly positive, which means that the values predicted by the model are, as a rule, slightly higher than the real ones (offset error). This result indicates that the additional fine tuning of the model is needed. Namely, the relatively small deviations of the predictive model results in relation to real results, with the tendency to "translatory skip" the real values, indicating that fuzzy values within the membership functions need to be additionally corrected. However, taking into account the good correlation between fuzzy rule base outputs with the real flotation system conditions, this is at the same time an indication that the performance of the model itself has "hit" its own limits. In this sense, hybridization of this fuzzy logic model with other soft computing methods is recommended.

By considering the data distribution in the range of $\pm$ 1 SDE, it was found that in this range lies 67.6% of the prediction error values for CCU, 74.7% for RCU and 71.2% for TCU.

Besides the absolute prediction error, one of the criteria for assessing model adequacy is the relative prediction error. This parameter can provide a clearer insight and additional data on the effectiveness of the predictive model, because it is used as a basis for comparing parameters that are expressed in different measurement units and different value ranges. Figure 16 presents the relative prediction errors of the CCU, RCU and TCU parameters of the PMM model.

By visual analysis of the charts in Figure 16, as well as consideration of the statistical parameters, it can be observed that the smallest relative prediction error is obtained when modeling RCU, and the highest when modeling TCU, which is consistent with their R^2.

The relative prediction error of RCU has the smallest standard deviation, and 82.1% of the results are in the range $\pm$ 1 SDE_r. When it comes to relative prediction errors of CCU and TCU, 73.6% and 79.0% of the results are within $\pm$ 1 SDE_r., respectively.

Table 9 shows that the results obtained by the PSM model are very similar to the PMM model results. The high values of determination coefficients indicate the existence of a strong relationship between the actual and predicted values of metallurgical indicators.

Prediction error diagrams (Figure 17) have shown small (more frequently) and larger (less frequently) deviations from the actual results. Margin errors (maximum and minimum) are also high, as in the previous case (Figure 15), but such extremes occur very rarely.

The prediction error trends of the copper content and recovery of the concentrate is almost identical to the trends shown in Figure 15.

Moreover, when it comes to the error of predicting the copper content in the tailings, the trend largely coincides with the corresponding trend of Figure 15. The only difference that is possible to observe is that a smaller number of error values are close to extremes. This leads to the conclusion that the deviations between the predicted and actual tailings grade are somewhat smaller, which also corresponds to the slightly higher value of the determination coefficient of the PSM model for the TCU variable.

Generally, for both models (PMM and PSM), the values of TCU prediction errors are mostly between $\pm$ 0.05% Cu, which is consistent with RMSE values (0.034 both, Table 9). It can be concluded that both models provided effective predictions, overall. As for the PMM model, the TCU prediction error is mostly positive, which indicates an offset error.

Similar to the PMM model, 67.7% of the prediction error values for CCU, 73.8% for RCU and 72.1% for TCU are in the range $\pm$ 1 SDE.

When considering the relative prediction error presented in Figure 18, it is also concluded that the results are very similar to the results of the PMM model.

In the range $\pm$ 1 SDE_r are 73.1% of the relative prediction error results for CCU, 82.1% for RCU and 79.4% for TCU (Figure 18).

3.2. Neural Network-Based Models

3.2.1. Model Performances

Three different models based on the principle of feed-forward backpropagation NN were trained. Model NN1 predicts copper content in the final concentrate, model NN2 predicts copper recovery in the final concentrate and model NN3 predicts copper content in the final tailings.

The architecture of the NN that gave the smallest Mean Square Error (MSE) of validation (best validation performance) was chosen as the most favorable predictive model. Mathematically, *MSE* can be defined as:

$$MSE = \frac{1}{n}\sum_{i=1}^{n}(X - Y)^2 \quad (8)$$

where X is the measured value, Y is the predicted value, and n is the number of samples.

The NN models consisting of 64, 43 and 24 neurons in the hidden layer gave the lowest mean squared error among all models studied for NN1, NN2 and NN3, respectively. The networks' performances in the training stage are shown in Figures 19–21.

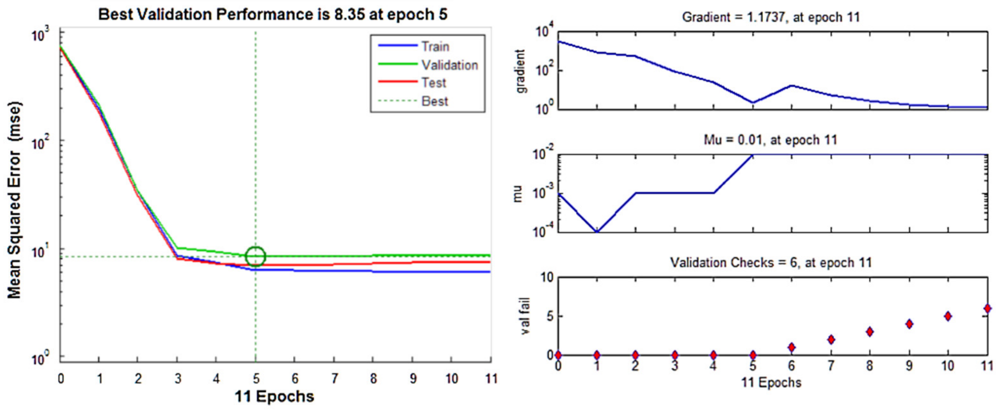

Figure 19. Training state and performance of the generated NN1 model for CCU.

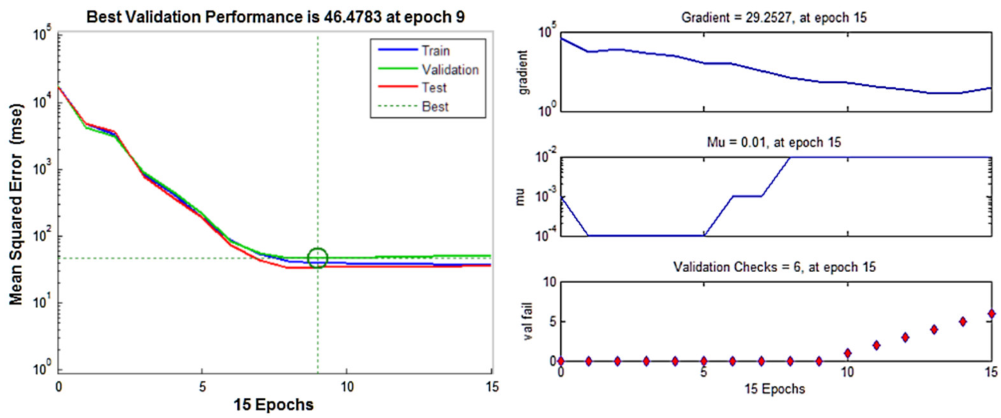

Figure 20. Training state and performance of the generated NN2 model for RCU.

Figure 19 demonstrates the MSE variation of the training, validation and testing stages versus the iteration number. As shown in this figure, the large values for the MSE were gradually reduced to a smaller value as the weights are updated. The training stage stopped at 5th epoch, i.e., after epochs 5, there was not a significant improvement in the performance of the model. The best validation performance was 8.35 at epoch 5, implying a good stable network behavior. Then, after six error iterations (validation checks), the process stopped at epoch 11. The similar explanation provided for Figure 19 can also be applied for Figures 20 and 21.

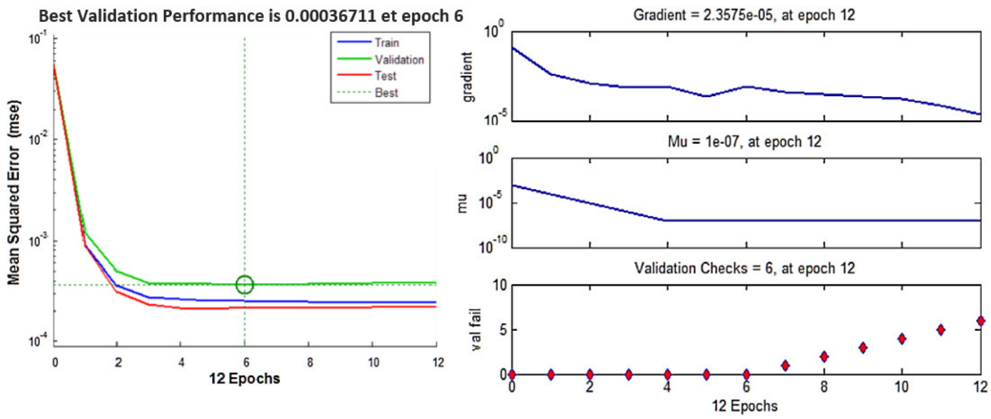

Figure 21. Training state and performance of the generated NN3 model for TCU.

One of the important phenomena that can be observed from the Figures 19–21 is that no overfitting occurred during training, testing and validation.

Overfitting can be spotted when the error on the training data decreases to a small value, but the error on the test/validation data increases to a large value. Some reasons for overfitting are: small size of the training dataset, very noisy dataset and complex ANN architecture [63].

When the network tries to learn from a small dataset, it will tend to have greater control over the dataset and to satisfy all the data points exactly. Therefore, the network is trying to memorize every single data point and failing to capture the general trend from the training dataset. In the observed case, a relatively large training dataset is applied, containing 1336 samples.

Overfitting also occurs when the model tries to make predictions on data that is very noisy, which results that the overfitted model is inaccurate, as the trend does not reflect the reality present in the data. By using the early stopping technique (small number of epochs), the network can be prevented from overfitting the noise in the data [63]. In the observed case, the number of epochs is relatively small, i.e., 11, 15 and 12 epochs for NN1, NN2 and NN3, respectively.

Increasing the number of hidden units and/or layers may lead to overfitting because it will make it easier for the neural network to memorize the training set, but to avoid generalization to unseen data. Therefore, a too large number of neurons in the hidden layer is undesirable. There is an empirical formula for the optimal number of hidden neurons (N_h) in the hidden layer [64]:

$$N_h = \frac{N_s}{\alpha(N_i + N_o)} \tag{9}$$

where N_i represents the number of input neurons, N_o is the number of output neurons, N_s is the number of samples in training dataset and α is the scaling factor, which takes values from 2 to 10.

If this formula is applied to the observed case, the number of hidden neurons should vary between 22 and 111. NN1, NN2 and NN3 models contain 64, 43 and 24 hidden neurons, respectively, which corresponds to the specified range. Since overfitting is not occurred, the numbers of hidden neurons are correctly chosen.

3.2.2. Predictive Abilities of NN-Based Models

The predicted results demonstrate the R^2 value 0.98 for CCU, 0.99 for RCU and 0.87 for TCU, demonstrating the success of the proposed NN models (Table 10). As it can be observed from Table 10, the RMSE between predicted and actual data by using NN models are very small, which means they can accurately predict the flotation performance indicators within the entire process variables' space.

Table 10. Statistical analysis of actual and predicted values using NN1, NN2 and NN3 models.

Statistical Parameters	Technological Indicator of the Flotation Process		
	CCU	RCU	TCU
R^2	0.982	0.994	0.867
RMSE	2.567	6.284	0.015
Mean of prediction error	−0.017	−0.338	0.0015
SDE	2.589	6.323	0.016
Maximum positive error (maximum)	10.933	44.501	0.043
Minimum positive error	0.00102	0.00694	0.000003
Minimum negative error	−0.00230	−0.01246	−0.00004
Maximum negative error (minimum)	−10.892	−16.341	−0.113
Mean of relative prediction error, μ_r	0.019	0.002	0.222
SDE_r	0.154	0.089	0.551

NN errors for the prediction of CCU, RCU and TCU are shown in Figure 22. It can be observed that these errors are mostly between ± 2.7% Cu and ± 5% for CCU and RCU, respectively. The prediction errors of the copper content and recovery in the final concentrate are very rarely out of range of ± 5% Cu and ± 10%, respectively. This is consistent with the RMSE values of 2.567 for NN1 and 6.284 for NN2 (Table 10).

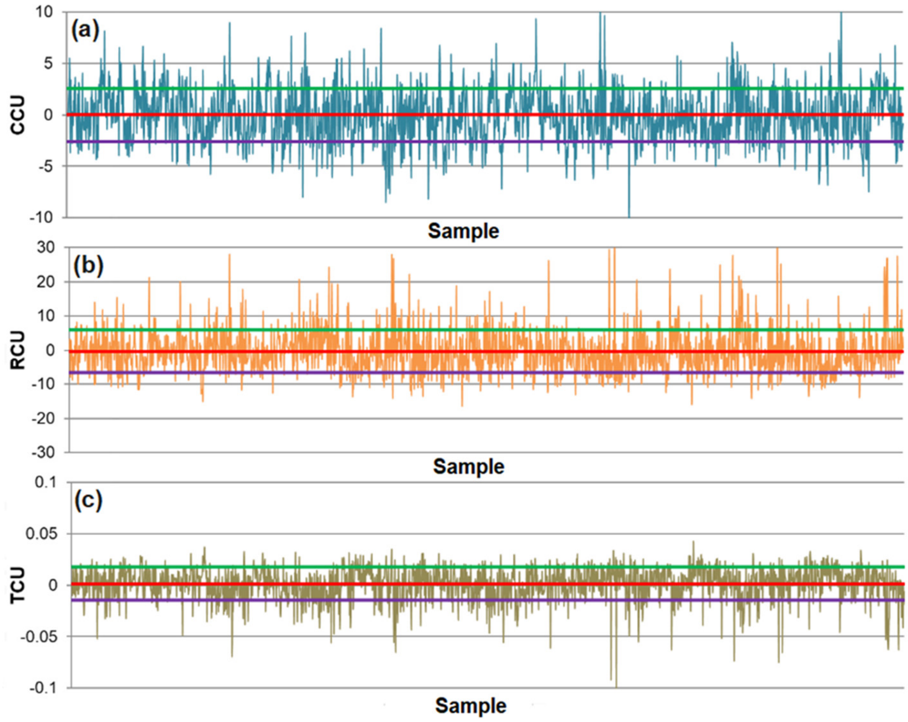

Figure 22. Prediction errors of technological indicators according to the (**a**) NN1, (**b**) NN2 and (**c**) NN3 models. The red line on the charts represents mean (μ), green line value μ + 1 SDE and purple line value μ − 1 SDE.

Analyzing the results obtained by the NN3 model from Figure 22, we explored that the prediction errors of the TCU mostly take values in the range of ± 0.016% Cu, which is consistent with its RMSE of 0.015 (Table 10). Examining the data distribution of the prediction error in the range of ± 1 SDE, it was found that 68.9%, 74.3% and 72.1% data lies within this range for CCU, RCU and TCU, respectively.

Figure 23 shows the relative error of the predictive models. Similar to the previous observations (for PMM and PSM), the smallest relative prediction error with the smallest standard deviation was obtained for the RCU variable. This is consistent with the highest coefficient of determination also achieved for the RCU (Table 10).

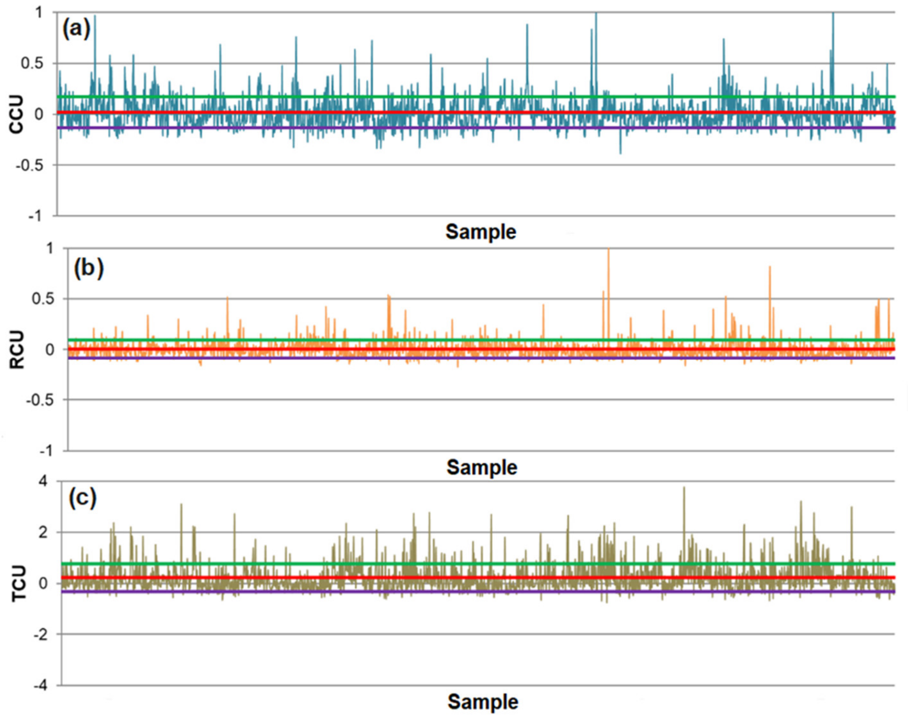

Figure 23. Relative prediction errors of technological indicators according to the (**a**) NN1, (**b**) NN2 and (**c**) NN3 models. The red line on the charts represents mean (μ_r), green line value μ_r + 1 SDE_r and violet line value $\mu_r - 1$ SDE_r.

The number of datum lying in the $\pm$ 1 SDE_r range is similar to the previous two models, and is 75.1% for the NN1 model, 81.4% for the NN2 model and 78.7% for the NN3 model.

In general, from the obtained results, it was found that the NN models are well fitting the real data and have the ability to predict the output data. It can be concluded that the NN models have good predictive properties, because of significant fluctuations in real process data. The validation set and test set had similar behavior with no occurrence of overfitting.

3.3. Summary Discussion

Comparative presentation of statistical parameters of every model is given in Figures 24–26.

According to Figure 24, the accuracy of the NN models is higher than the accuracy of fuzzy models. The dependent variables (CCU, RCU and TCU) are better explained in the NN models than in the fuzzy models by the independent variables (FCU, PXR, FRT, PHR and PXS), since the determination coefficients are higher and the RMSE are significantly smaller. It can be clearly observed that models based on NN demonstrate the best predictive abilities, while both fuzzy models demonstrate very similar performances. Therefore, practically there is no difference in the utilization of either the Mamdani or Takagi Sugeno inference system under a wide range of operation conditions.

A similar conclusion can be made based on the results shown in Figures 25 and 26. The smallest standard deviations of predictive error (both absolute and relative) have neural networks when it comes to all output variables. A low standard deviation indicates that the values tend to be close to the mean (also called the expected value) of the set, while a high standard deviation indicates that the values are spread over a wider range.

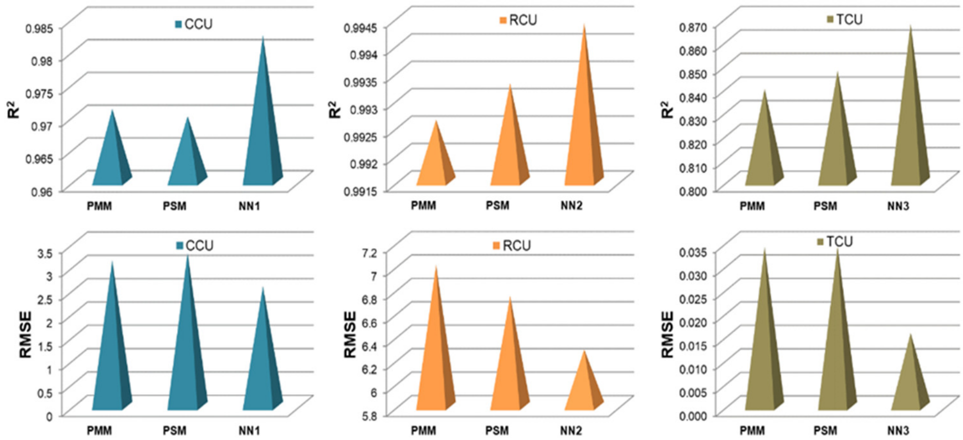

Figure 24. Comparison of fuzzy and ANN modeling results: R^2 and RMSE.

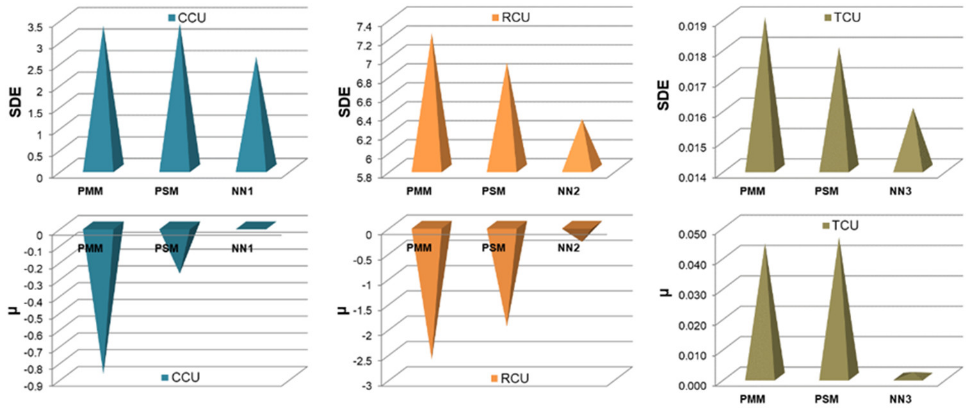

Figure 25. Comparison of fuzzy and ANN modeling results: SDE and μ.

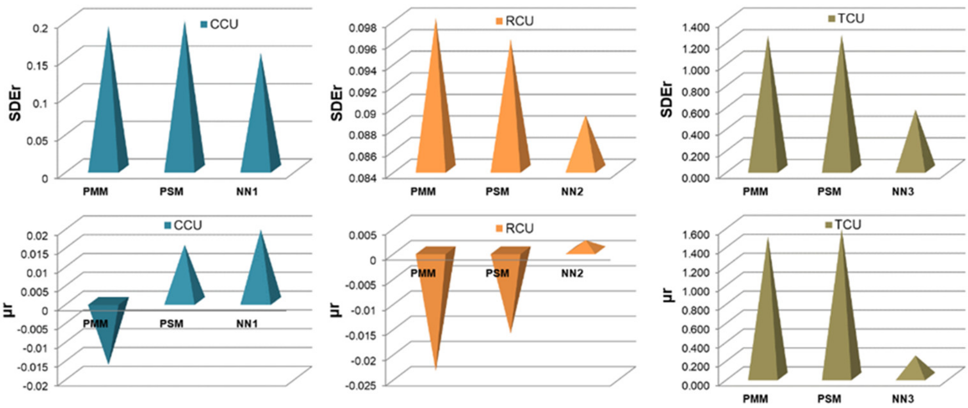

Figure 26. Comparison of fuzzy and ANN modeling results: SDE_r and μ_r.

By analyzing the statistical parameters of the relative error, it is observed that the RCU variable has the smallest standard deviations (SDE_r) in all models, which corresponds to the highest coefficients of determination for RCU variable in all models. Further, the variable TCU has the highest standard deviations of the relative prediction error, which also corresponds to the smallest values of R^2 in relation to CCU and RCU (Tables 8–10).

The means of the absolute errors for CCU and RCU variables are negative, which indicates that the models have a greater tendency to predict values that are less than the real ones. On the other hand, the means of errors for TCU are positive, which indicates that the models have a tendency to predict higher values from real ones. In accordance with the second observation are offset errors in the Figures 15c and 17c.

This study demonstrates that the developed models can be used as new tools to estimate the performance of the flotation circuit based on operational conditions, which are readily available at an industrial plant. Due to the dynamic nature and variations in real data, building an appropriate model for the prediction of flotation process in an industrial plant is a challenging task. More complex algorithms always require a larger amount of data. The sample size would depend on the number of input features and degree of nonlinearity between input and predicted variables (nature of the problem) [65]. In this paper, more than 1900 samples were used to capture the complexity of the process. The results indicate that the proposed NN and fuzzy models are able to predict the performance indicators of the flotation process in an industrial plant based on a large dataset with a high accuracy. The main reason why these models are more precise than some other presented models is that such models reported in the past were based on a small data set [2,28,66].

4. Conclusions

In this study, the metallurgical parameters of an industrial copper flotation plant were predicted by two fuzzy logic models (Mamdani and Takagi-Sugeno) and three back-propagation neural network (BPNN) models. Since the grade and recovery of concentrate are essential factors for decision making and control of the industrial flotation plant, their predictive model accuracy is very important. Therefore, a large dataset (1910 samples) was collected by daily/shiftly process monitoring during the multiannual plant's operation. The most effective parameters, namely copper grade in the ore feed, collector dosage in the rougher and the scavenger circuits, slurry pH in the rougher circuit and frother consumption, were selected and used in all models. The performance of each model was evaluated by well-known evaluation criteria, RMSE, R^2.and SD of prediction error. Based on the obtained results, the following can be concluded:

- The purpose of modeling the production process in the Veliki Krivelj plant is the possibility of implementing the obtained models into an automatic control system of this process. This system would include the application of controllers based on fuzzy logic or artificial neural networks.
- The NN and fuzzy logic models provided effective estimations due to the high R^2 and low RMSE values. However, the NN models were slightly more robust and accurate in predicting the values of metallurgical factors compared to the fuzzy logic models. The RMSE values of the NN models for the prediction of copper grade and recovery of the final concentrate were 2.567 and 6.284, respectively.
- Neural networks have the smallest standard deviations of the absolute and relative prediction error for all output variables.
- The differences between predicted and actual values are relatively small for all models. The significant deviations between actual and predicted values most likely occurred due to the fluctuations in real process data that can be caused by various factors, such as changing process dynamics due to the downtime of the plant, oscillations in the process parameters that were considered constant during modeling, changes in the reagents' quality, changes in process water quality, human factor, etc.
- The highest determination coefficients between actual and predicted values were obtained when modeling the copper recovery in the final concentrate, and the lowest when modeling the copper content in the final tailings. This can be applied to all models. The reason may lie in that the values of copper content in tailings vary in a relatively narrow range in relation to quality and recovery. Therefore, it may happen that the influences of completely different values of input parameters are integrated through very similar or the same copper contents in tailings, without this being taken into account during modeling. Such a situation could significantly affect the determination coefficient. Moreover, possible imperfections during tailings'

sampling (which are particularly linked to instabilities in the operation of the plant) should not be ignored, because the copper content in the samples is extremely low, and therefore proper sampling is of crucial importance for obtaining the precise chemical composition of the tailings.
- In accordance with the previous statement, the smallest standard deviations of the relative prediction error were obtained with the models that predict Cu recovery in the concentrate, and the largest with the models that predict Cu content in the tailings.
- By comparing the results of Mamdani and Takagi Sugeno fuzzy inference systems, it can be inferred that they demonstrate very similar predictive performance.
- Further research will be focused on the inclusion of other independent variables into the models, as well as on the modeling of individual parts of the flotation process depending on the availability (i.e., continual measurement) of process data to evaluate whether prediction results are improved or not.
- Sensitivity analysis of models, especially regarding the parameters considered constant, can be very helpful when it comes to improving the performances of the models and also represents the topic of future research.
- The application of more advanced software tools, as well as other soft computing methods, can also be effective in modeling such systems based on relatively large sets of input and output data.

Author Contributions: Conceptualization, I.J.; Methodology, I.J., F.N., D.K. and V.C.; Validation, F.N.; Investigation, I.J. and F.N.; Resources, I.J.; Data curation, D.K., V.C. and D.U.; Writing—original draft preparation, I.J. and F.N.; Writing—review and editing, D.K. and V.C.; Visualization, D.U.; Supervision, D.K., V.C. and D.U. All authors have read and agreed to the published version of the manuscript.

Funding: This work was financially supported by the Ministry of Education, Science and Technological Development of the Republic of Serbia, Grant No. 451-03-68/2022-14/200052.

Acknowledgments: We thank the Ministry of Education, Science and Technological Development of the Republic of Serbia.

Conflicts of Interest: The authors declare no conflict of interest.

Appendix A

During the observed period, in which measurement and data collection was carried out, the control and regulation system in the Veliki Krivelj flotation plant mainly relied on a manual mode of operation. This means that there is no fully automated and continuous monitoring of process parameters, but the role of controller is performed by experienced plant operators. In order to maintain the technological process in the stable state, the following technological parameters were measured and regulated:

- Particle size analysis of grinding products;
- Pulp density;
- Pulp level;
- Pulp pH value;
- Reagents' consumption.

Particle size distribution of the grinding product is one of the parameters that gives insight into the liberation degree of the mineral raw material. In order to determine the particle size distribution of the finally ground product, a sample of the hydrocyclone overflow is taken, and then sieved in the laboratory on the sieve with 0.074 mm aperture. The percentage mass content of the −0.074 mm class should be within a certain range (i.e., 58%–60%). If this content is lower than required, a correction is made at the feed to the rod mill by reducing the ore processing capacity or reducing the grinding pulp density within the prescribed range. If this content is higher than required, the ore processing capacity increases. When it comes to the overflow of the hydrocyclone in regrinding circuit, the regulation of the particle size distribution is conducted by reducing the amount of water (if the overflow is too coarse) or by increasing the amount of water (if the overflow is too fine) that is added to the regrinding mill.

In addition to the control of the finally ground product, if necessary, control of the grinding product of the rod mill, ball mill and regrinding mill is also carried out. Since the process is continuous and there is a need for quick reaction and process corrections, it is necessary to perform visual controls during the work. These controls are performed every hour and consist of rinsing a sample of the hydrocyclone overflow on the mining pan.

Pulp density has a significant impact on the grinding, classification and flotation process. The appropriate pulp density in the mills ensures the maximum capacity of the mill, while in the classifier (hydrocyclone), it affects the coarseness of the overflow. The optimal pulp density in the flotation cells provides adequate conditions for the optimization of the copper mineral flotation process.

Pulp density control is performed at various points in the process, such as for example, rod and ball mill discharges, hydrocyclone underflow and overflow, etc. Pulp density is determined by the glass pycnometer method in the laboratory. However, due to the timely reaction to changes in pulp density values in the process, it is necessary to perform a quick control of the same in the flotation plant. This procedure is performed by measuring the full "Denver" pycnometer on a "Denver" scale every 1–2 h.

Regulation of the pulp density is conducted by changing the amount of water added at certain points of the process or by changing the ore processing capacity. Water is added to the process manually, by means of a valve that corresponds to the given segment of the process in which the regulation is carried out.

The optimum value of the ***pulp level*** ensures the optimum time required for the hydrophobic mineral particles to adhere to the air bubbles. Regulation of the pulp level is done manually—by raising the plugs (when it is necessary to decrease the pulp level) or by lowering the plugs (when it is necessary to increase the pulp level), which are located in the boxes of the flotation machines.

The optimal ***pH value of the pulp*** creates optimal conditions for collector action on the surfaces of the mineral particles, as well as the selectivity of the flotation process. The pH value is measured with pH-meters whose electrodes are immersed in the hydrocyclone overflows. These values are read on the control panel display.

In addition, the pH values of all three cleaning tails are also determined. Samples are taken manually, and the pH is determined with manual pH-meters or the pulp titration method in the laboratory (this method is based on determining free lime in the clear part of the solution. The volumetric quantity of titrant (in this case HCl) needed to react with all $Ca(OH)_2$ in the solution (end point of the titration) is measured, according to the equation $Ca(OH)_2 + 2HCl = CaCl_2 + 2H_2O$).

To regulate the pH value of the pulp, lime is used, which is added to the process in the form of lime milk (6% aqueous solution of calcium oxide). When it comes to the grinding process, reducing or increasing the dose of milk of lime, depending on the desired pH value of the pulp, is conducted from the control panel, by adjusting the clearance of the pneumatic valves located at each dosing point. The regulation of lime milk consumption in each stage of cleaning is conducted manually.

Reagents are, as is known, one of the key elements for the success of the copper flotation process. Control of the reagent dosage (collector and frother) is performed by measuring the flow of reagents (which is read in the control room) and calculating their consumption per ton of processed ore.

Potassium ethyl xanthate (PEX) is used as collector and dosed into the process in the form of a 10% solution. PEX is added only to the roughing and scavenging circuit. The regulation of collector consumption is a complex task that depends on a number of factors in the plant. First of all, the information obtained from the mining pit about the ore mineralogical composition and copper content is considered. In addition, a visual analysis of the ground material, concentrate and tailings is performed by washing them on the mining pan every hour (the analysis of intermediate products is also performed in this way, but with a lower frequency of testing). The appearance of the flotation froth in terms of its color, bubble size, mineralization, etc., is also monitored.

Therefore, there are a number of factors that indicate whether it is necessary to increase or decrease the dose of the collector. Experienced plant operators recognize these indicators and take appropriate management action accordingly. Regulation of the collector consumption is conducted manually, using the valves located at each dosing point.

Dowfroth 250 is used as a frother and added to the process in liquid form, concentrated. Frother is only added in the agitation stage, just before the roughing. Its consumption primarily depends on the stability of the flotation froth (i.e., whether the froth "grows" or is prone to collapse), then on the presence of alumina in the feed, etc. The frother flow is regulated in one place, by means of a manual valve.

Besides the mentioned parameters, which are controlled and regulated directly in the "Veliki Krivelj" flotation plant, particle size distribution of the finally crushed ore is determined daily, which can indicate the efficiency of the crushing process and the eventual need to regulate the processing capacity in grinding. In addition, the copper content in the feed ore, concentrate and tailings is determined by chemical analysis. Samples for chemical analysis are taken every hour, and from the hourly increments, shift composite samples are formed. Based on results of chemical analyses, feed capacity and concentrate quantity, the recovery of copper in concentrate is calculated.

Data on the input parameters of the technological process, as well as data on the concentration products, are collected by daily monitoring and stored in the record documentation. Data are stored for each individual shift as a shift average.

For the purposes of model development, a two-and-a-half-year period of continuous plant production was chosen, with a total of 2553 shift data available to the authors. These data are arranged in a time-line order. However, considering that during the plant operation there is a stoppage due to various factors (such as device failures, the need for overhaul and lack of ore from the open pit), the analysis found that data are missing for certain shifts, either completely or partially. Moreover, due to errors that may occur during sampling, or due to the imperfection of chemical analyses, imperfection of measuring instruments, imperfection of calculations (human factor), etc., some shift data contained illogicalities in the sense of extremely low or extremely high values of process parameters. Such shift data were also eliminated from the primary dataset, so that the final and complete dataset contained 1910 shift data. The time-line sequence in the data arrangement is preserved.

Analyzing these final datasets, it was still possible to notice data scattering, as well as relatively large differences between minimum and maximum values for certain variables (e.g., recovery). Still, one of the modeling goals was to use a maximal quantity of industrial data and to, however is possible, follow the process continuity and the changes that occur over time. Therefore, these scatterings were considered normal during the industrial process, with the level of error in the process parameters determination up to 10%, according to the experiences of process and chemical engineers.

Appendix B

Appendix B.1. Input Datasets

Input datasets, as well as their distributions, are given in Figures A1–A10.

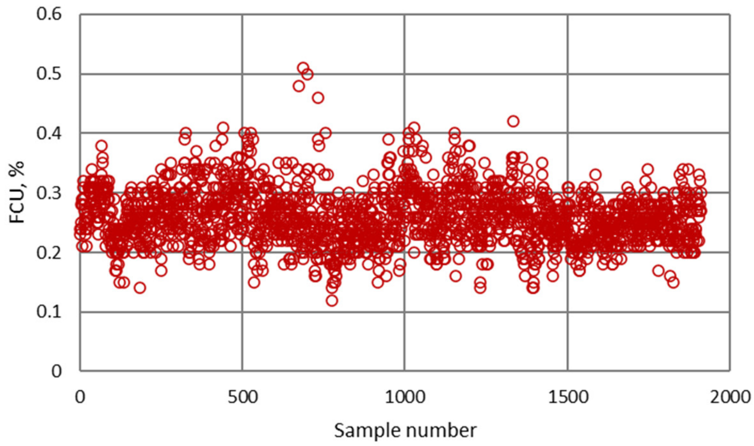

Figure A1. Copper content in feed (FCU)—input dataset.

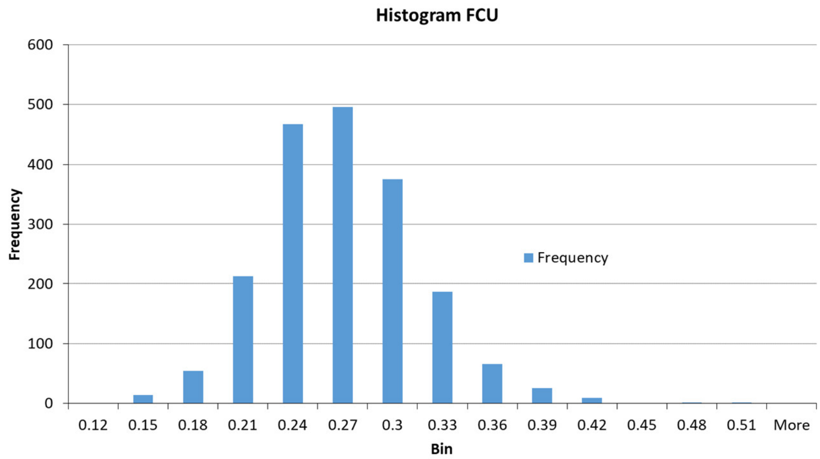

Figure A2. Copper content in feed (FCU)—dataset distribution.

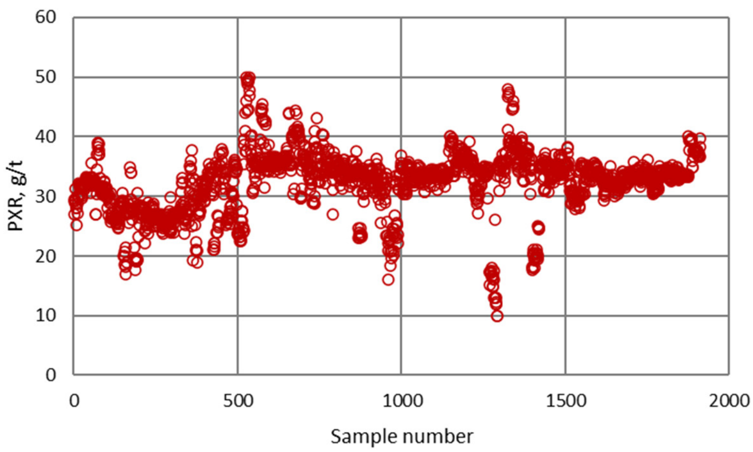

Figure A3. Collector consumption in rougher flotation stage (PXR)—input dataset.

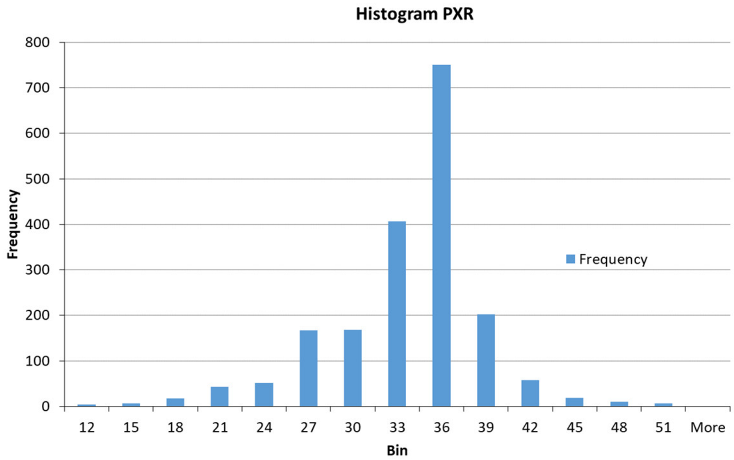

Figure A4. Collector consumption in rougher flotation stage (PXR)—dataset distribution.

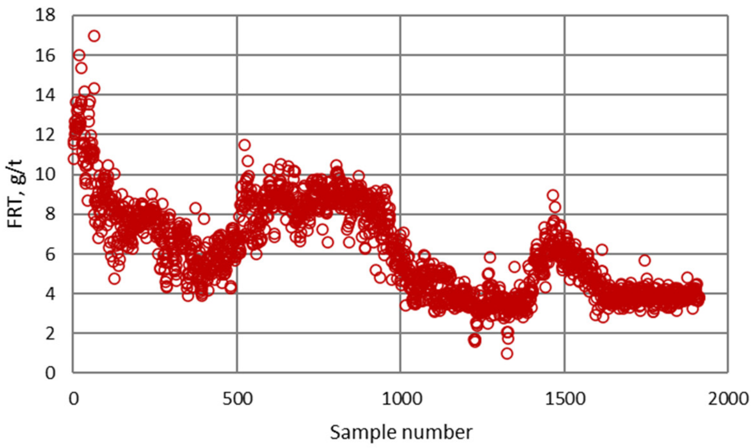

Figure A5. Frother consumption (FRT)—input dataset.

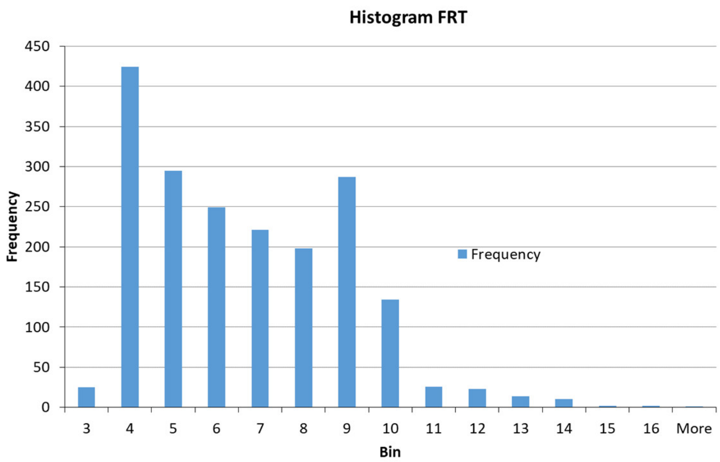

Figure A6. Frother consumption (FRT)—dataset distribution.

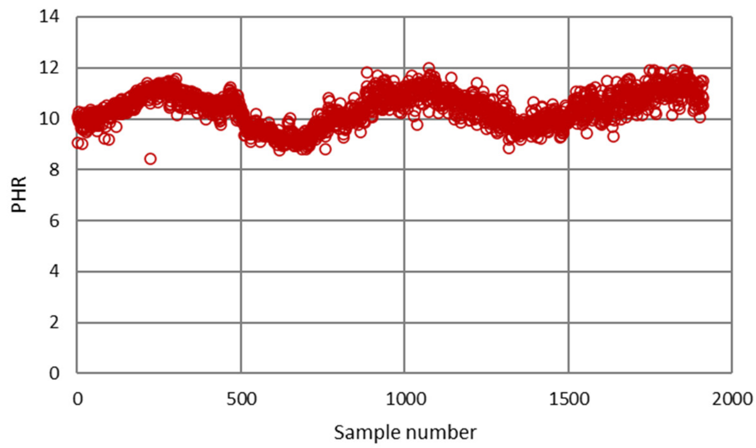

Figure A7. pH value of the pulp in rougher flotation stage (PHR)—input dataset.

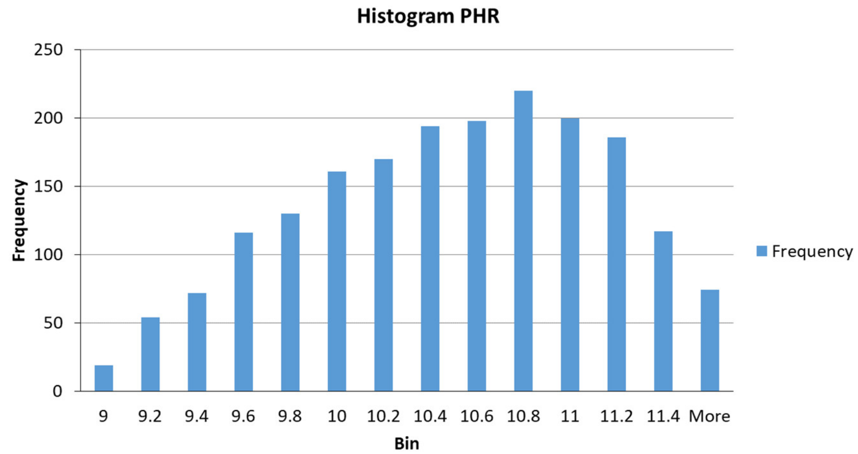

Figure A8. pH value of the pulp in rougher flotation stage (PHR)—dataset distribution.

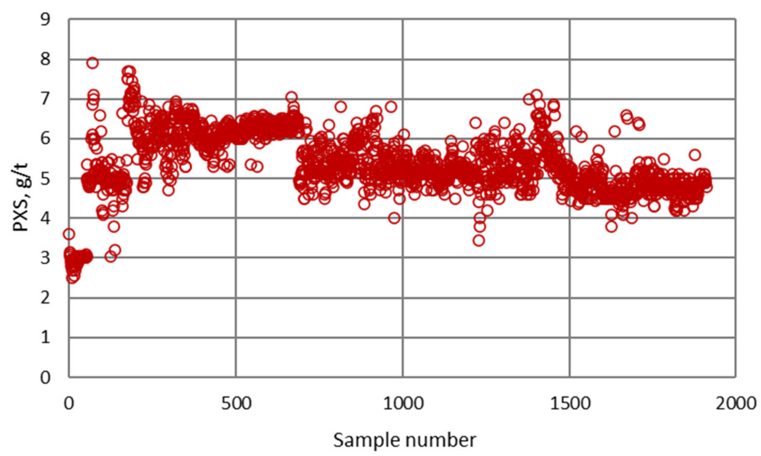

Figure A9. Collector consumption in scavenger flotation stage (PXS)—input dataset.

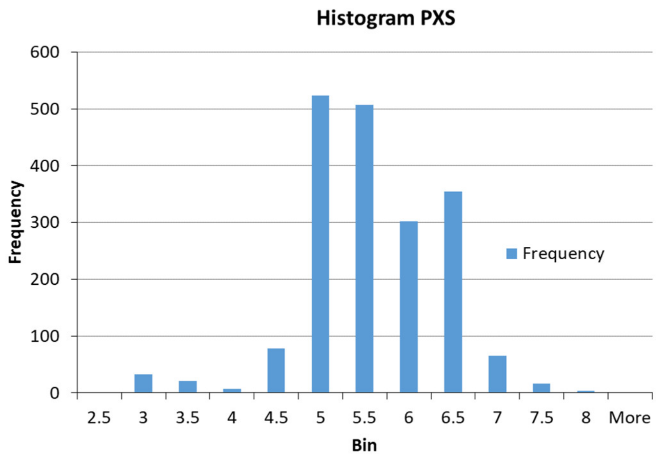

Figure A10. Collector consumption in scavenger flotation stage (PXS)—dataset distribution.

Appendix B.2. Output Datasets, Training, Testing and Validation Datasets

Distributions of output datasets are given in Figures A11–A13. Since all the data from the training testing and validation sets can be observed, the entire output datasets are not shown here.

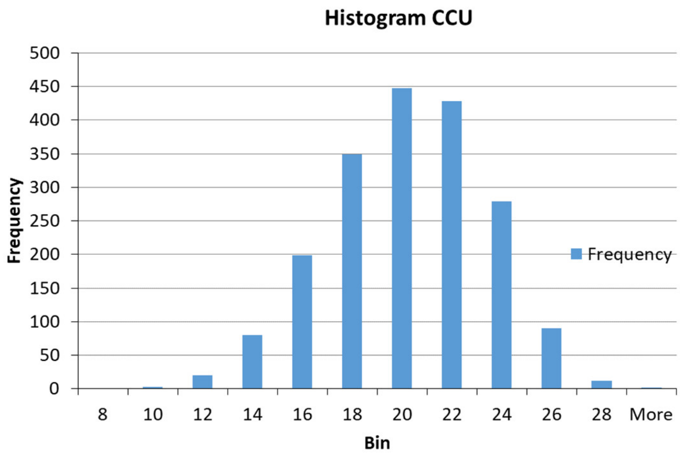

Figure A11. Copper content in final concentrate (CCU)—dataset distribution.

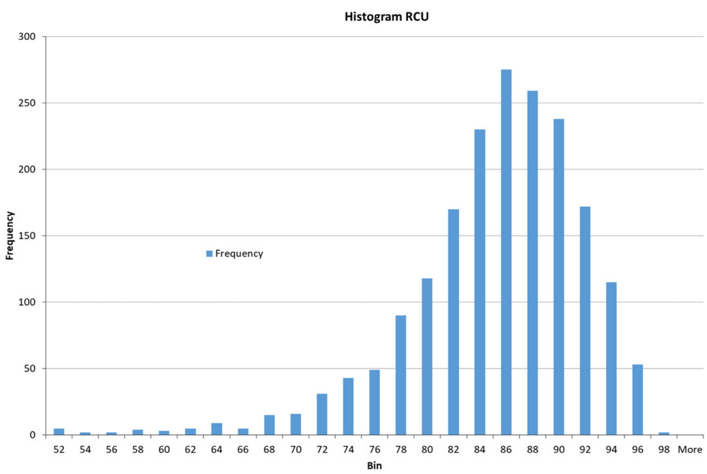

Figure A12. Copper recovery in final concentrate (RCU)—dataset distribution.

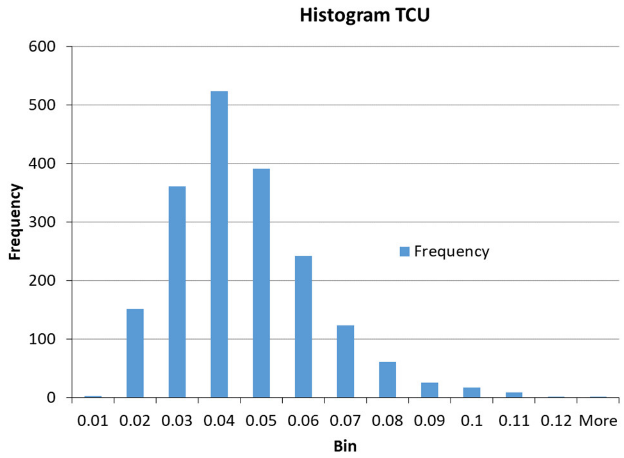

Figure A13. Copper content in final tailings (TCU)—dataset distribution.

Appendix B.2.1. Fuzzy Logic Model Based on Mamdani Inference System—PMM

Training and testing datasets of this model are selected on the following way:

- Data from every even shift (955 in total) are determined for training,
- Data from every odd shift (955 in total) are determined for testing.

Based on training results, the additional adjusting of fuzzy numbers within membership functions is performed. Fuzzy logic model based on the Takagi-Sugeno inference system (PSM) is obtained only by transformation of PMM to compare the results.

Training Datasets

Information about the PMM model training dataset is shown in Figures A14–A19 and in the Table A1.

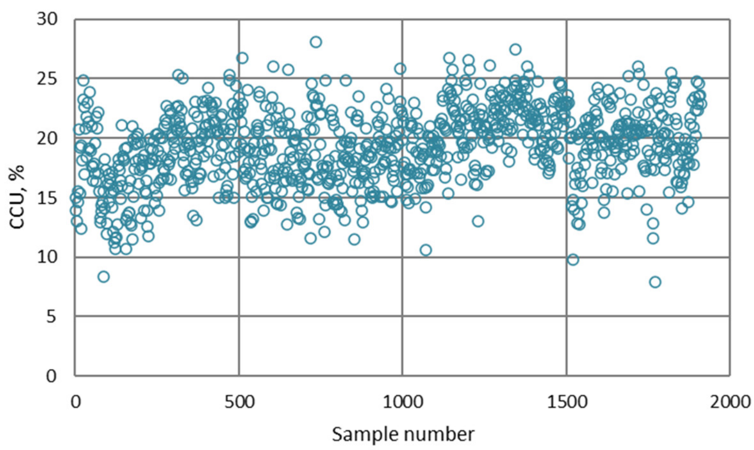

Figure A14. PMM model—training dataset for CCU output variable.

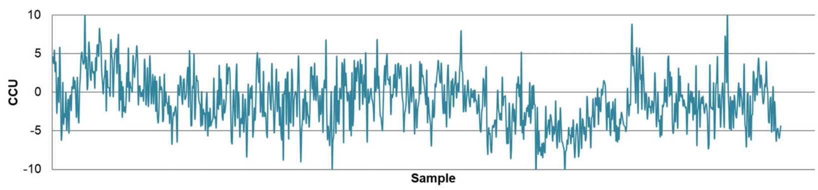

Figure A15. Prediction error of PMM model training dataset for CCU output variable.

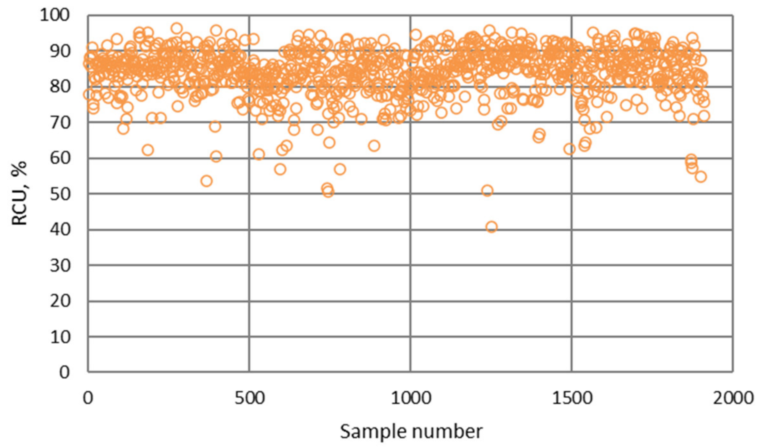

Figure A16. PMM model—training dataset for RCU output variable.

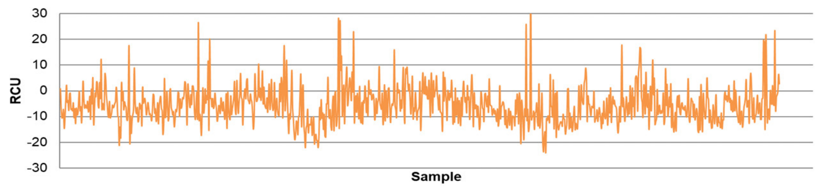

Figure A17. Prediction error of PMM model training dataset for RCU output variable.

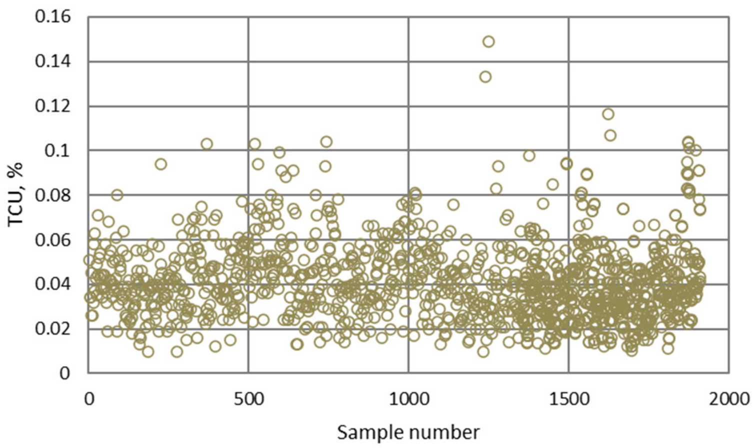

Figure A18. PMM model—training dataset for TCU output variable.

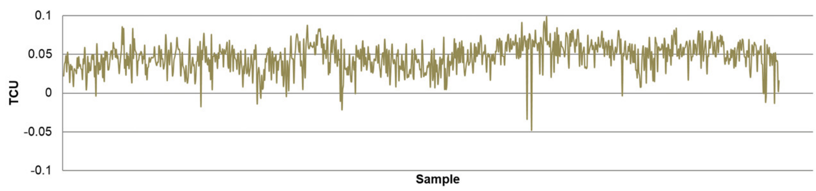

Figure A19. Prediction error of PMM model training dataset for TCU output variable.

Table A1. Regression statistics parameters of PMM model training dataset.

Statistical Parameters	Technological Indicator of the Flotation Process		
	CCU	RCU	TCU
R^2	0.971	0.992	0.851
RMSE	3.096	6.681	0.034

Testing Datasets

Information about the PMM model testing datasets is shown in Figures A20–A25 and in the Table A2.

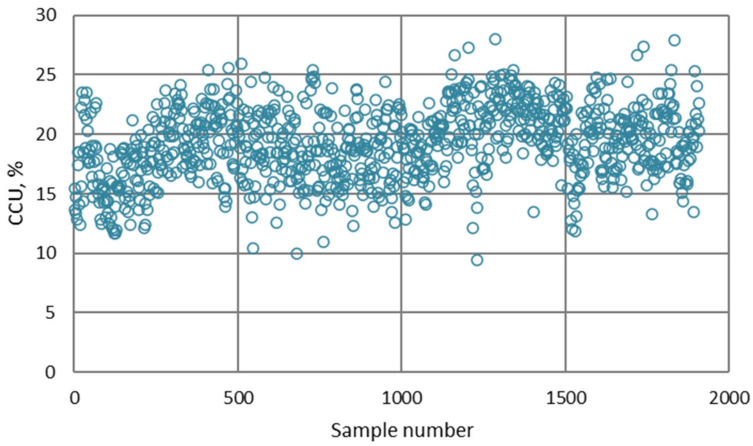

Figure A20. PMM model—testing dataset for CCU output variable.

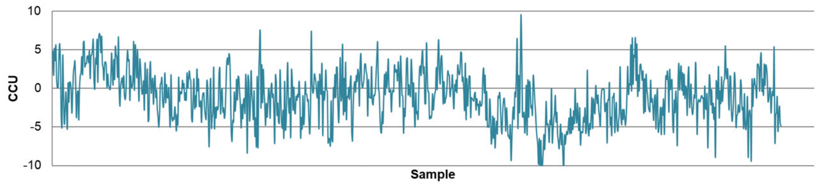

Figure A21. Prediction error of PMM model testing dataset for CCU output variable.

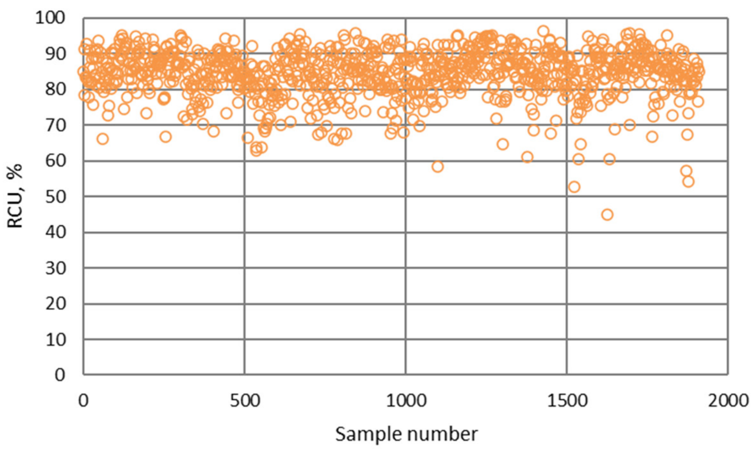

Figure A22. PMM model—testing dataset for RCU output variable.

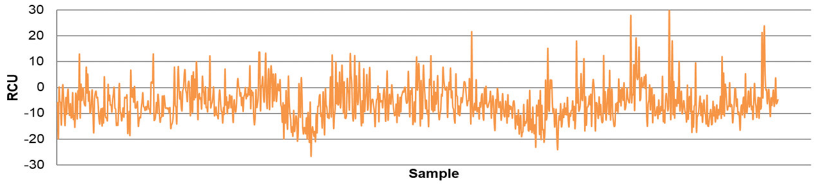

Figure A23. Prediction error of PMM model testing dataset for RCU output variable.

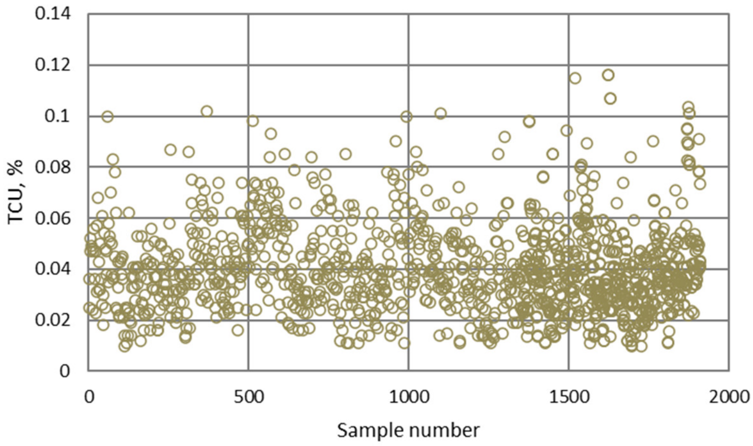

Figure A24. PMM model—testing dataset for TCU output variable.

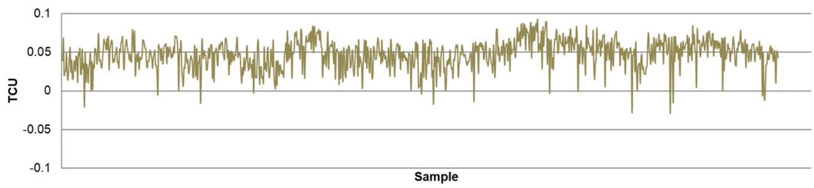

Figure A25. Prediction error of PMM model testing dataset for TCU output variable.

Table A2. Regression statistics parameters of PMM model testing dataset.

Statistical Parameters	Technological Indicator of the Flotation Process		
	CCU	RCU	TCU
R^2	0.972	0.993	0.840
RMSE	3.049	6.613	0.035

Appendix B.2.2. Artificial Neural Network-Based Model for CCU Prediction—NN1

Training, testing and validation data sets of this model are randomly chosen by the network in the following way:

- A total of 60% of the data (1336 in total) are determined for training;
- A total of 15% of the data (287 in total) are determined for testing;
- A total of 15% of the data (287 in total) are determined for validation.

Information about the NN1 model training, testing and validation datasets is shown in Figures A26–A31 and in the Table A3.

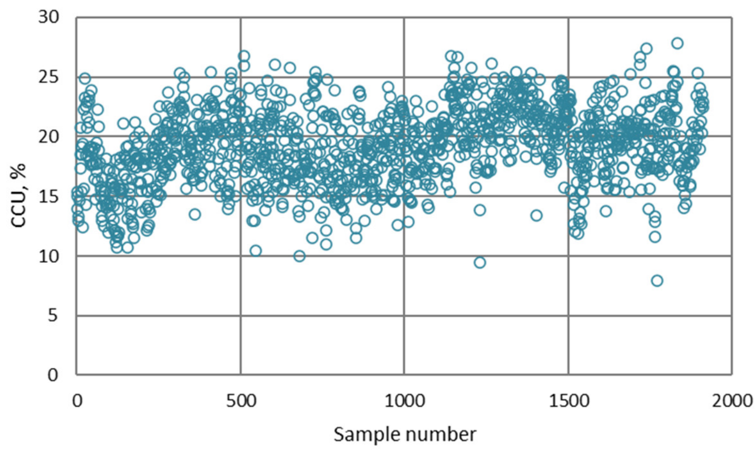

Figure A26. NN1 model—training dataset.

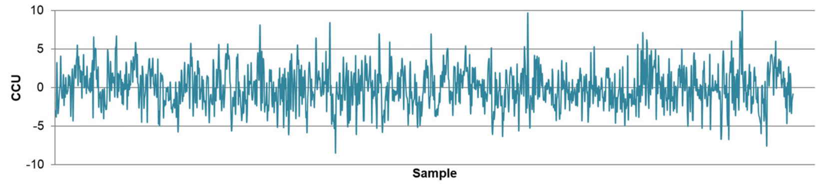

Figure A27. Prediction error of NN1 model training dataset.

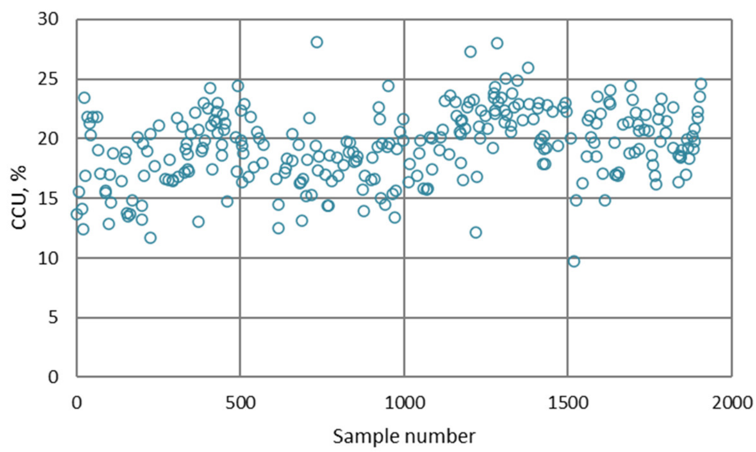

Figure A28. NN1 model—testing dataset.

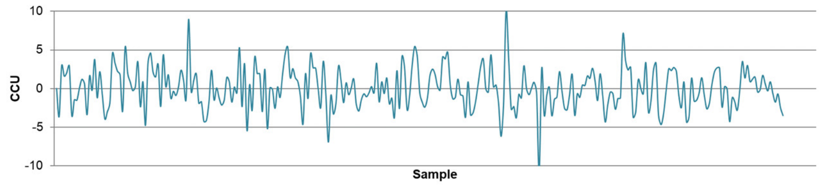

Figure A29. Prediction error of NN1 model testing dataset.

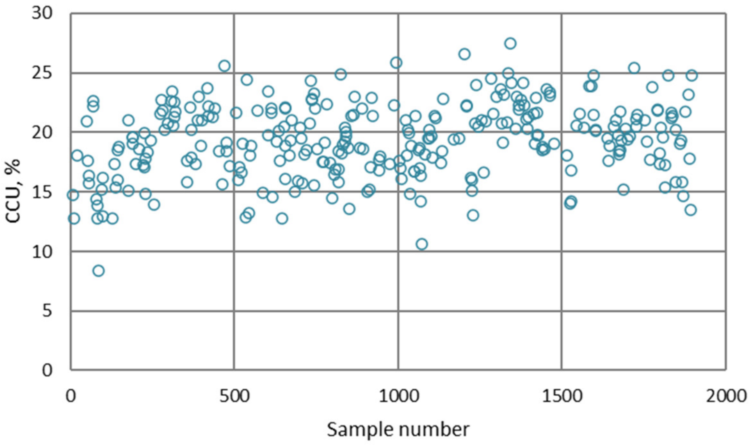

Figure A30. NN1 model—validation dataset.

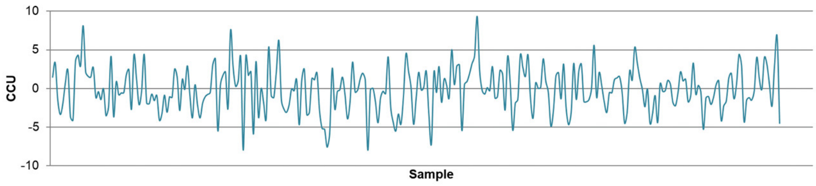

Figure A31. Prediction error of NN1 model validation dataset.

Table A3. Regression statistics parameters of NN1 model datasets.

Statistical Parameters	CCU		
	Training	Testing	Validation
R^2	0.983	0.981	0.978
RMSE	2.489	2.635	2.854

Appendix B.2.3. Artificial Neural Network-Based Model for RCU Prediction—NN2

Training, testing and validation data sets of this model are randomly chosen by the network in the following way (same as for NN1):

- A total of 60% of the data (1336 in total) are determined for training;
- A total of 15% of the data (287 in total) are determined for testing;
- A total of 15% of the data (287 in total) are determined for validation.

Information about the NN2 model training, testing and validation datasets is shown in Figures A32–A37 and in the Table A4.

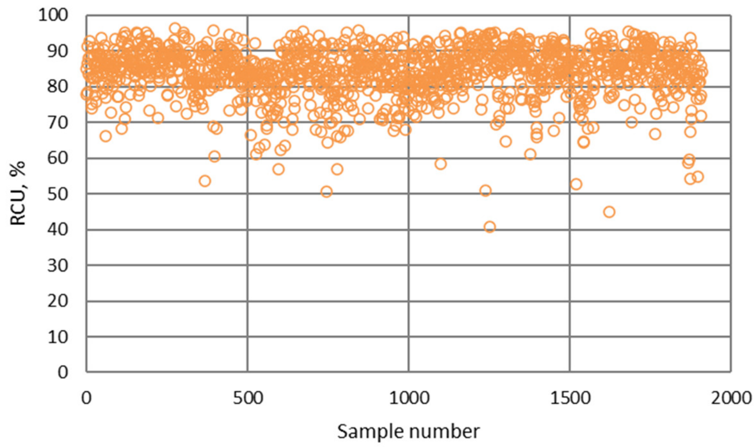

Figure A32. NN2 model—training dataset.

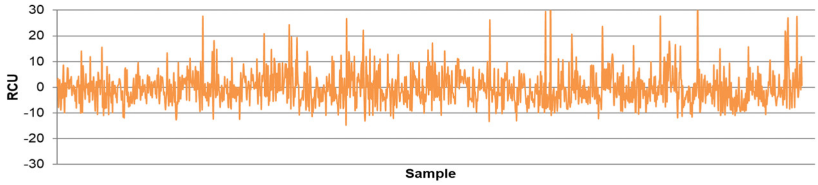

Figure A33. Prediction error of NN2 model training dataset.

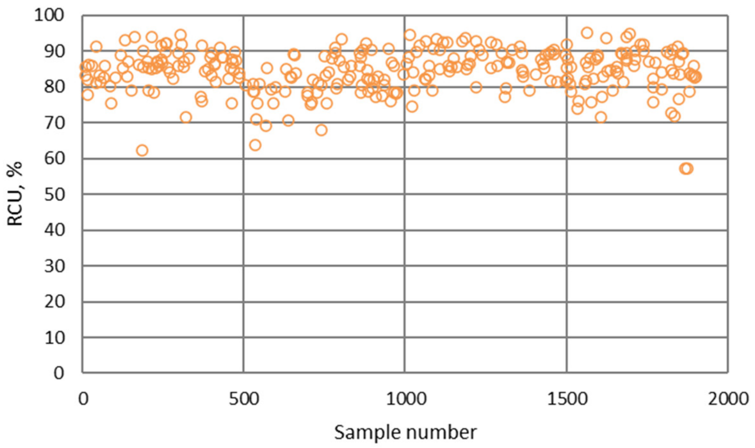

Figure A34. NN2 model—testing dataset.

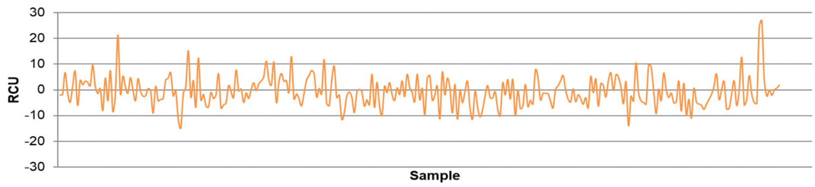

Figure A35. Prediction error of NN2 model testing dataset.

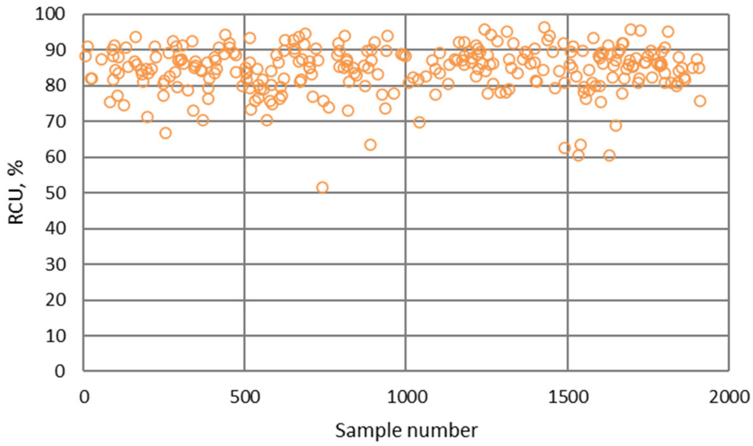

Figure A36. NN2 model—validation dataset.

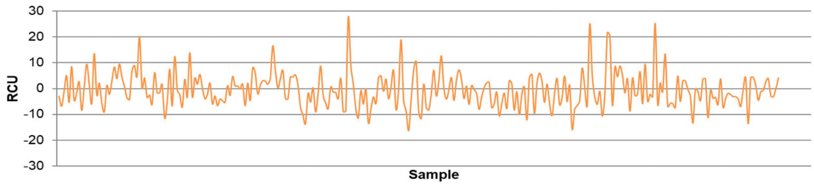

Figure A37. Prediction error of NN2 model validation dataset.

Table A4. Regression statistics parameters of NN1 model datasets.

Statistical Parameters	RCU		
	Training	Testing	Validation
R^2	0.994	0.995	0.993
RMSE	6.291	5.762	6.767

Appendix B.2.4. Artificial Neural Network-Based Model for TCU Prediction—NN3

Training, testing and validation data sets of this model are randomly chosen by the network in the following way (same as for NN1 and NN2):

- A total of 60% of the data (1336 in total) are determined for training;
- A total of 15% of the data (287 in total) are determined for testing;
- A total of 15% of the data (287 in total) are determined for validation.

Information about the NN3 model training, testing and validation datasets is shown in Figures A38–A43 and in the Table A5.

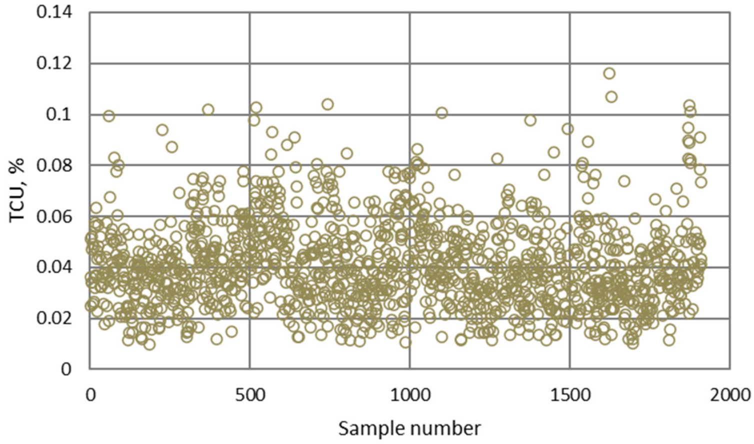

Figure A38. NN3 model—training dataset.

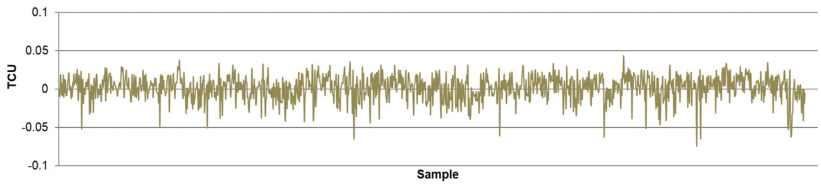

Figure A39. Prediction error of NN3 model training dataset.

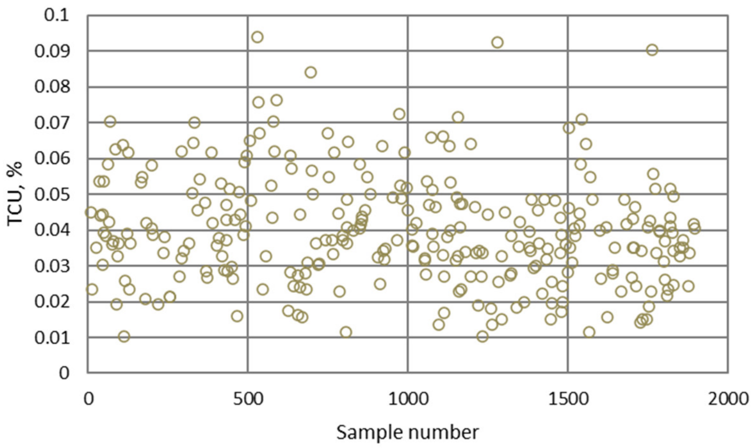

Figure A40. NN3 model—testing dataset.

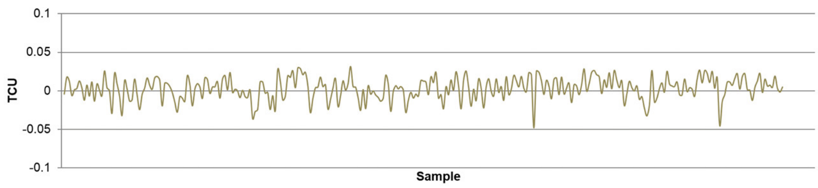

Figure A41. Prediction error of NN3 model testing dataset.

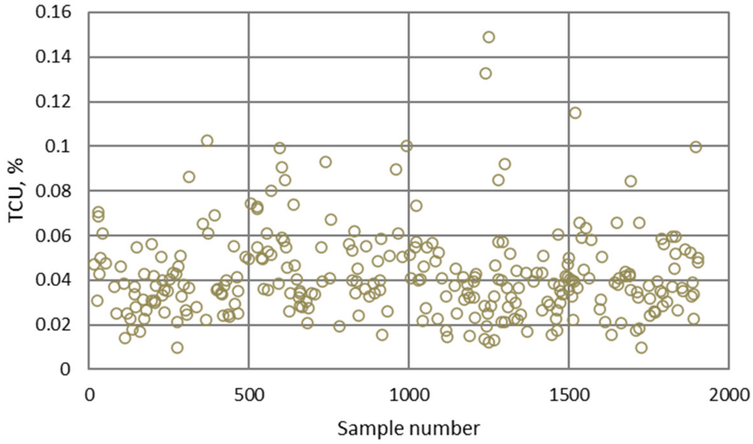

Figure A42. NN3 model—validation dataset.

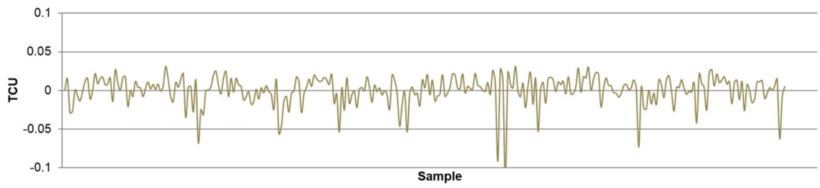

Figure A43. Prediction error of NN3 model validation dataset.

Table A5. Regression statistics parameters of NN3 model datasets.

Statistical Parameters	RCU		
	Training	Testing	Validation
R^2	0.873	0.884	0.829
RMSE	0.015	0.014	0.017

References

1. Jovanović, I.; Magdalinović, N.; Kržanović, D.; Rajković, R. Comparative analysis of AI models in the modeling of flotation process. In *Mining and Metallurgy Engineering Bor 3-4/2018*; Mining and Metallurgy Engineering Bor: Bor, Serbia, 2018; pp. 27–32, ISSN 2334-8836.
2. Nakhaei, F.; Sam, A.; Mosavi, M.R.; Zeidabadi, S. Prediction of copper grade at flotation column concentrate using artificial neural network. In Proceedings of the IEEE 10th International Conference on Signal Processing Proceedings, Beijing, China, 24–28 October 2010; pp. 1421–1424.
3. Quintanilla, P.; Neethling, S.J.; Brito-Parada, P.R. Modelling for froth flotation control: A review. *Miner. Eng.* **2021**, *162*, 106718. [CrossRef]
4. Jovanović, I. Model Inteligentnog Sistema Adaptivnog Upravljanja Procesom Prerade Rude. Ph.D. Thesis, Rudarsko-geološki Fakultet, Belgrade, Serbia, 2016; p. 217. (In Serbian)
5. Jovanović, I.; Miljanović, I.; Jovanović, T. Soft computing-based modeling of flotation processes—A review. *Miner. Eng.* **2015**, *84*, 34–63. [CrossRef]
6. Cisternas, L.A.; Lucay, F.A.; Botero, Y.L. Trends in Modeling, Design, and Optimization of Multiphase Systems in Minerals Processing. *Minerals* **2020**, *10*, 22. [CrossRef]
7. Dos Santos, N.A.; Savassi, O.; Peres, A.E.C.; Martins, A.H. Modelling flotation with a flexible approach—Integrating different models to the compartment model. *Miner. Eng.* **2014**, *66–68*, 68–76. [CrossRef]
8. Seppälä, P.; Sorsa, A.; Paavola, M.; Ruuska, J.; Remes, A.; Kumar, H.; Lamberg, P.; Leiviskä, K. Development and calibration of a dynamic flotation circuit model. *Miner. Eng.* **2016**, *96–97*, 168–176. [CrossRef]
9. Suazo, C.J.; Kracht, W.; Alruiz, O.M. Geometallurgical modelling of the Collahuasi flotation circuit. *Miner. Eng.* **2010**, *23*, 137–142. [CrossRef]
10. Al-Thyabat, S. On the optimization of froth flotation by the use of artificial neural network. *J. China Univ. Min. Technol.* **2008**, *18*, 418–426. [CrossRef]

11. Farghaly, M.; Serwa, A.; Ahmed, M. Optimizing the Egyptian Coal Flotation Using an Artificial Neural Network. *J. Min. World Express* **2012**, *1*, 27–33.
12. Jorjani, E.; Mesroghli, S.; Chelgani, S.C. Prediction of operational parameters effect on coal flotation using artificial neural network. *J. Univ. Sci. Technol. Beijing* **2008**, *15*, 528–533. [CrossRef]
13. Nakhaei, F.; Mosavi, M.R.; Sam, A.; Vaghei, Y. Recovery and grade accurate prediction of pilot plant flotation column concentrate: Neural network and statistical techniques. *Int. J. Miner. Process.* **2012**, *110–111*, 140–154. [CrossRef]
14. Nakhaei, F.; Irannajad, M. Comparison between neural networks and multiple regression methods in metallurgical performance modeling of flotation column. *Physicochem. Probl. Miner. Process.* **2013**, *49*, 255–266.
15. Nakhaei, F.; Irannajad, M. Forecasting grade and recovery of flotation column concentrate using radial basis function and layer recurrent neural networks. *AWERProcedia Inf. Technol. Comput. Sci.* **2013**, *4*, 454–473.
16. Jahedsaravani, A.; Marhaban, M.H.; Massinaei, M. Application of statistical and intelligent techniques for modeling of metallurgical performance of a batch flotation process. *Chem. Eng. Commun.* **2016**, *203*, 151–160. [CrossRef]
17. Massinaei, M.; Sedaghati, M.R.; Rezvani, R.; Mohammadzadeh, A.A. Using data mining to assess and model the metallurgical efficiency of a copper concentrator. *Chem. Eng. Commun.* **2014**, *201*, 1314–1326. [CrossRef]
18. Zhang, Y.; Chen, H.; Yang, B.; Fu, S.; Yu, J.; Wang, Z. Prediction of phosphate concentrate grade based on artificial neural network modeling. *Results Phys.* **2018**, *11*, 625–628. [CrossRef]
19. Abdulhussein, S.A.; Alwared, A.I. The use of Artificial Neural Network (ANN) for modeling of Cu (II) ion removal from aqueous solution by flotation and sorptive flotation process. *Environ. Technol. Innov.* **2019**, *13*, 353–363. [CrossRef]
20. Gholami, A.; Movahedifar, M.; Khoshdast, H.; Hassanzadeh, A. Hybrid Serving of DOE and RNN-Based Methods to Optimize and Simulate a Copper Flotation Circuit. *Minerals* **2022**, *12*, 857. [CrossRef]
21. Aldrich, C.; Marais, C.; Shean, B.J.; Cilliers, J.J. Online monitoring and control of froth flotation systems with machine vision: A review. *Int. J. Miner. Process.* **2010**, *96*, 1–13. [CrossRef]
22. Marais, C.; Aldrich, C. The estimation of platinum flotation grade from froth image features by using artificial neural networks. *J. South. Afr. Inst. Min. Metall.* **2011**, *111*, 81–85.
23. Marais, C.; Aldrich, C. Estimation of platinum flotation grades from froth image data. *Miner. Eng.* **2011**, *24*, 433–441. [CrossRef]
24. Jahedsaravani, A.; Marhaban, M.H.; Massinaei, M. Prediction of the metallurgical performances of a batch flotation system by image analysis and neural networks. *Miner. Eng.* **2014**, *69*, 137–145. [CrossRef]
25. Hosseini, M.R.; Haji Amin Shirazi, H.; Massinaei, M.; Mehrshad, N. Modeling the Relationship between Froth Bubble Size and Flotation Performance Using Image Analysis and Neural Networks. *Chem. Eng. Commun.* **2015**, *202*, 911–919. [CrossRef]
26. Wang, J.-S.; Han, S.; Shen, N.-N.; Li, S.-X. Features Extraction of Flotation Froth Images and BP Neural Network Soft-Sensor Model of Concentrate Grade Optimized by Shuffled Cuckoo Searching Algorithm. *Sci. World J.* **2014**, *2014*, 208094. [CrossRef]
27. Haiyang, Z.; Yali, K.; Guanghui, W.; Li, J. Soft Sensor Model for Coal Slurry Ash Content Based on Image grey characteristics. *Int. J. Coal Prep. Util.* **2014**, *34*, 24–37. [CrossRef]
28. Nakhaei, F.; Irannajad, M.; Mohammadnejad, S. Column flotation performance prediction: PCA, ANN and image analysis-based approaches. *Physicochem. Probl. Miner. Process.* **2019**, *55*, 1298–1310.
29. Nakhaei, F.; Irannajad, M.; Mohammadnejad, S. A comprehensive review of froth surface monitoring as an aid for grade and recovery prediction of flotation process. Part A: Structural features. *Energy Sources Part A Recovery Util. Environ. Eff.* **2019**. [CrossRef]
30. Zhang, H.; Tang, Z.; Xie, Y.; Gao, X.; Chen, Q.; Gui, W. Long short-term memory-based grade monitoring in froth flotation using a froth video sequence. *Miner. Eng.* **2021**, *160*, 106677. [CrossRef]
31. Fu, Y.; Aldrich, C. Flotation froth image recognition with convolutional neural networks. *Miner. Eng.* **2019**, *132*, 183–190. [CrossRef]
32. Pu, Y.; Szmigiel, A.; Chen, J.; Apel, D.B. FlotationNet: A hierarchical deep learning network for froth flotation recovery prediction. *Powder Technol.* **2020**, *375*, 317–326. [CrossRef]
33. Zarie, M.; Jahedsaravani, A.; Massinaei, M. Flotation froth image classification using convolutional neural networks. *Miner. Eng.* **2020**, *155*, 106443. [CrossRef]
34. Wen, Z.; Zhou, C.; Pan, J.; Nie, T.; Zhou, C.; Lu, Z. Deep learning-based ash content prediction of coal flotation concentrate using convolutional neural network. *Miner. Eng.* **2021**, *174*, 107251. [CrossRef]
35. Gao, X.; Tang, Z.; Xie, Y.; Zhang, H.; Gui, W. A layered working condition perception integrating handcrafted with deep features for froth flotation. *Miner. Eng.* **2021**, *170*, 107059. [CrossRef]
36. Jahan, A.; Edwards, K.L.; Bahraminasab, M. Multi-Attribute Decision-Making for Ranking of Candidate Materials. In *Multi-criteria Decision Analysis for Supporting the Selection of Engineering Materials in Product Design*, 2nd ed.; Jahan, A., Edwards, K.L., Bahraminasab, M., Eds.; Butterworth-Heinemann: Oxford, UK, 2016; pp. 81–126.
37. Naderloo, L.; Alimardani, R.; Omid, M.; Sarmadian, F.; Javadikia, P.; Torabi, M.Y.; Alimardani, F. Application of ANFIS to predict crop yield based on different energy inputs. *Measurement* **2012**, *45*, 1406–1413. [CrossRef]
38. Amiryousefi, M.R.; Mohebbi, M.; Khodaiyan, F.; Asadi, S. An empowered adaptive neuro-fuzzy inference system using self-organizing map clustering to predict mass transfer kinetics in deep-fat frying of ostrich meat plates. *Comput. Electron. Agric.* **2011**, *76*, 89–95. [CrossRef]

39. Sitorus, F.; Brito-Parada, P.R. Equipment selection in mineral processing—A sensitivity analysis approachfor a fuzzy multiple criteria decision making model. *Miner. Eng.* **2020**, *150*, 106261. [CrossRef]
40. Zhang, W.; Liu, D.; Du, Y.; Liu, R.; Wang, D.; Yu, L.; Wen, S. Mill Feed Control System and Algorithm Based on Python. *Minerals* **2022**, *12*, 804. [CrossRef]
41. Jovanović, I.; Nešković, J.; Petrović, S.; Milanović, D. A hybrid approach to modeling the flotation process from the "Veliki Krivelj" plant. In *Mining and Metallurgy Engineering Bor 1-2/2018*; Mining and Metallurgy Engineering Bor: Bor, Serbia, 2018; pp. 1–10. ISSN 2334-8836.
42. Lott, G.D.; Da Silva, M.T.; Cota, L.P.; Guimarães, F.G.; Euzébio, T.A.M. Fuzzy Decision Support System for the Calibration of Laboratory-Scale Mill Press Parameters. *IEEE Access* **2021**, *9*, 24901–24912. [CrossRef]
43. Carvalho, M.T.; Durão, F. Performance of a flotation column fuzzy controller. In *Computers and Computational Engineering in Control*; Mastorakis, N.E., Ed.; World Scientific and Engineering Society Press: Athens, Greece, 1999; pp. 220–225.
44. Carvalho, M.T.; Durão, F. Control of a flotation column using fuzzy logic inference. *Fuzzy Sets Syst.* **2002**, *125*, 121–133. [CrossRef]
45. Vieira, S.M.; Sousa, J.M.C.; Durão, F.O. Fuzzy modelling strategies applied to a column flotation process. *Miner. Eng.* **2005**, *18*, 725–729. [CrossRef]
46. Liao, Y.; Liu, J.; Wang, Y.; Cao, Y. Simulating a fuzzy level controller for flotation columns. *Min. Sci. Technol.* **2011**, *21*, 815–818. [CrossRef]
47. Jahedsaravani, A.; Mehrshad, N.; Massinaei, M. Fuzzy-based modeling and control of an industrial flotation column. *Chem. Eng. Commun.* **2014**, *201*, 896–908.
48. Zhou, K.; Zhou, X. Adaptive fuzzy local ternary pattern for mineral flotation froth image edge detection. *IFAC Pap.* **2018**, *51*, 235–240. [CrossRef]
49. Liang, Y.; He, D.; Su, X.; Wang, F. Fuzzy distributional robust optimization for flotation circuit configurations based on uncertainty theories. *Miner. Eng.* **2020**, *156*, 106433. [CrossRef]
50. Ali, S. Mathematical Models for the Efficiency of Flotation Process for North Waziristan Copper. Ph.D. Thesis, University of Education, Lahore, Pakistan, 2007, 2007; p. 167.
51. Yang, L.; Liu, T.; Ren, W.; Sun, W. Fuzzy Neural Network for Studying Coupling between Drilling Parameters. *ACS Omega* **2021**, *6*, 24351–24361. [CrossRef]
52. Zadeh, L.A. A new direction in AI: Toward a computational theory of perceptions. *AI Mag.* **2001**, *22*, 73.
53. Latha, B.; Senthilkumar, V. Analysis of thrust force in drilling glass fiber-reinforced plastic composites using fuzzy logic. *Mater. Manuf. Process.* **2009**, *24*, 509–516. [CrossRef]
54. Şahin, M.; Erol, R. Prediction of Attendance Demand in European Football Games: Comparison of ANFIS, Fuzzy Logic, and ANN. *Comput. Intell. Neurosci.* **2018**, *2018*, 5714872. [CrossRef]
55. Lerkkasemsan, N.; Achenie, L.E. Pyrolysis of biomass–fuzzy modeling. *Renew. Energy* **2014**, *66*, 747–758. [CrossRef]
56. Bhowmik, S.; Panua, R.; Ghosh, S.K.; Paul, A.; Debroy, D. Prediction of performance and exhaust emissions of diesel engine fuelled with adulterated diesel: An artificial neural network assisted fuzzy-based topology optimization. *Energy Environ.* **2018**, *29*, 1413–1437. [CrossRef]
57. Ghodrati, S.; Nakhaei, F.; VandGhorbany, O.; Hekmati, M. Modeling and optimization of chemical reagents to improve copper flotation performance using response surface methodology. *Energy Sources Part A Recovery Util. Environ. Eff.* **2020**, *42*, 1633–1648. [CrossRef]
58. Asghari, M.; Nakhaei, F.; VandGhorbany, O. Copper recovery improvement in an industrial flotation circuit: A case study of Sarcheshmeh copper mine. *Energy Sources Part A Recovery Util. Environ. Eff.* **2019**, *41*, 761–778. [CrossRef]
59. Ćalić, N. *Teorijski Osnovi Pripreme Mineralnih Sirovina*; Rudarsko-geološki fakultet Beograd—Faculty of Mining and Geology: Belgrade, Serbia, 1990; p. 496. (In Serbian)
60. Jassbi, J.; Alavi, S.H.; Serra, P.J.A.; Ribeiro, R.A. Transformation of a Mamdani FIS to First Order Sugeno FIS. In Proceedings of the IEEE International Conference on Fuzzy Systems, London, UK, 23–26 July 2007; pp. 5–10.
61. Nakhaei, F.; Sam, A.; Mosavi, M.R. Concentrate Grade Prediction in an Industrial Flotation Column using the Artificial Neural Network. *Arab. J. Sci. Eng.* **2013**, *38*, 1011–1023. [CrossRef]
62. Nakhaei, F.; Irannajad, M. Application and comparison of RNN, RBFNN and MNLR approaches on prediction of flotation column performance. *Int. J. Min. Sci. Technol.* **2015**, *25*, 983–990. [CrossRef]
63. Ying, X. An Overview of Overfitting and its Solutions. *J. Phys. Conf. Ser.* **2019**, *1168*, 022022. [CrossRef]
64. Available online: https://towardsdatascience.com/the-secret-neural-network-formula-70b41f0da767 (accessed on 20 October 2020).
65. Sarker, I.H. Deep Learning: A Comprehensive Overview on Techniques, Taxonomy, Applications and Research Directions. *SN Comput. Sci.* **2021**, *2*, 420. [CrossRef] [PubMed]
66. Nikolić, I.; Jovanović, I.; Mihajlović, I.; Miljanović, I. Analiza proizvodnje koncentrata bakra sistemskim pristupom (Analysis of copper concentrate production by systemic approach). *Bakar* **2016**, *40*, 33–50. (In Serbian)